JACS
JOURNAL OF THE AMERICAN CHEMICAL SOCIETY
pubs.acs.org/JACS
Article

Ionizable Lipid Nanoparticles for *In Vivo* mRNA Delivery to the Placenta during Pregnancy

Kelsey L. Swingle, Hannah C. Safford, Hannah C. Geisler, Alex G. Hamilton, Ajay S. Thatte, Margaret M. Billingsley, Ryann A. Joseph, Kaitlin Mrksich, Marshall S. Padilla, Aditi A. Ghalsasi, Mohamad-Gabriel Alameh, Drew Weissman, and Michael J. Mitchell*

Cite This: https://doi.org/10.1021/jacs.2c12893

ABSTRACT: Ionizable lipid nanoparticles (LNPs) are the most clinically advanced nonviral platform for mRNA delivery. While they have been explored for applications including vaccines and gene editing, LNPs have not been investigated for placental insufficiency during pregnancy. Placental insufficiency is caused by inadequate blood flow in the placenta, which results in increased maternal blood pressure and restricted fetal growth. Therefore, improving vasodilation in the placenta can benefit both maternal and fetal health. Here, we engineered ionizable LNPs for mRNA delivery to the placenta with applications in mediating placental vasodilation. We designed a library of ionizable lipids to formulate LNPs for mRNA delivery to placental cells and identified a lead LNP that enables *in vivo* mRNA delivery to trophoblasts, endothelial cells, and immune cells in the placenta. Delivery of this top LNP formulation encapsulated with VEGF-A mRNA engendered placental vasodilation, demonstrating the potential of mRNA LNPs for protein replacement therapy during pregnancy to treat placental disorders.

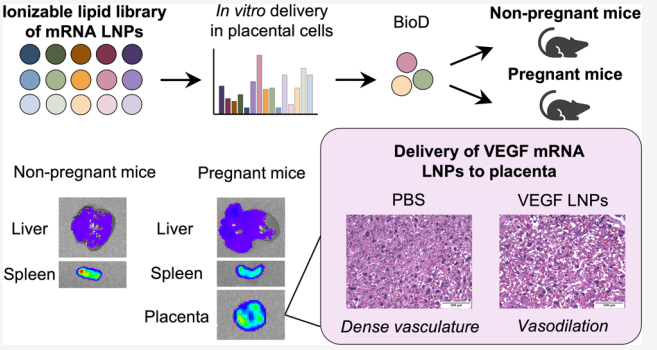

1. INTRODUCTION

Viral and nonviral nucleic acid delivery approaches have been explored for a variety of clinical applications, including vaccines, protein and enzyme replacement therapies, and gene editing technologies.[1,2] Viral platforms for nucleic acid delivery require genomic integration and therefore result in permanent gene expression.[3] However, these platforms pose risks associated with immunogenicity and ectopic genomic integration, which can be particularly harmful in gene editing applications.[4,5] Nonviral approaches include the delivery of therapeutic messenger RNA (mRNA), which does not require nuclear transport and initiates transient protein expression in the cytosol.[5,6] mRNA faces several delivery challenges *in vivo*, including rapid degradation by nucleases and poor cellular uptake, due to its large size and negative charge.[2,7] Drug delivery platforms such as lipid nanoparticles (LNPs) can address these challenges, as they have demonstrated efficient cellular uptake and potent mRNA delivery *in vivo*.[8−13] Currently, LNPs are the most clinically advanced nonviral drug delivery platform for nucleic acid therapeutics. Specifically, LNPs are utilized for Moderna and Pfizer/BioNTech's COVID-19 mRNA vaccines and Intellia's gene editing therapies for congenital disorders.[14−16] For these reasons, many groups including our own are exploring LNP-mediated mRNA delivery for novel applications.

To our knowledge, LNP-mediated nucleic acid therapy has been relatively unexplored for applications during pregnancy including placental disorders. The placenta is an organ that is fetal in origin and develops rapidly during gestation to supply nutrients and oxygen to the fetus.[17,18] Insufficient vasodilation in the placenta can result in disorders such as pre-eclampsia, which affects 3−8% of all pregnancies.[18−20] During pre-eclampsia, placental vasodilation is compromised and maternal blood pressure rises in an effort to continue providing nutrients and oxygen to the fetus.[18] In severe cases, fetal growth restriction (FGR) develops, which is characterized by abnormally low fetal growth rates. FGR is the leading cause of stillbirth and prematurity worldwide, as the only curative treatment option for pre-eclampsia and FGR involves delivering the fetus regardless of viability and gestational age.[20]

To address pre-eclampsia and FGR, several groups have developed gene therapies to improve placental vasodilation and angiogenesis. This has been done by either upregulating

Received: December 6, 2022

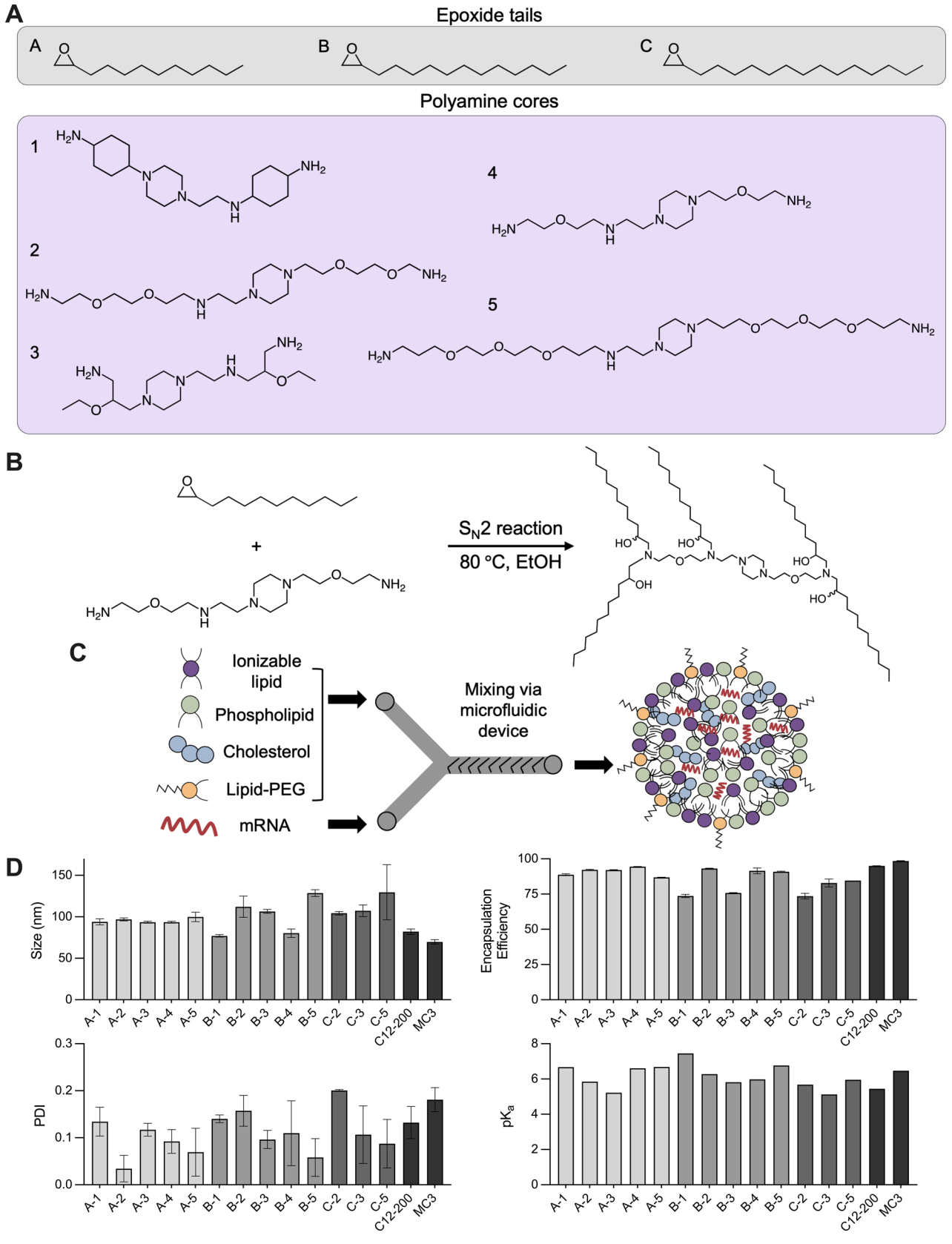

Figure 1. Overview of the ionizable lipid library and LNP formulation and characterization. (A) Structures of the three epoxide tails—C12 (A), C14 (B), and C16 (C)—as well as the five polyamine cores—1, 2, 3, 4, and 5—that make up the library of ionizable lipids screened in the LNP library. (B) Synthesis of ionizable lipid A4 via S_N2 reaction. (C) Formulation of LNPs via microfluidic mixing of an ethanol phase containing ionizable lipid, phospholipid, cholesterol, and lipid-PEG and an aqueous phase containing mRNA. (D) Hydrodynamic diameter, polydispersity index (PDI), mRNA encapsulation efficiency, and pK_a characterization of the LNP library. Data are reported as mean ± standard deviation (n = 3 observations).

https://doi.org/10.1021/jacs.2c12893
J. Am. Chem. Soc. XXXX, XXX, XXX−XXX

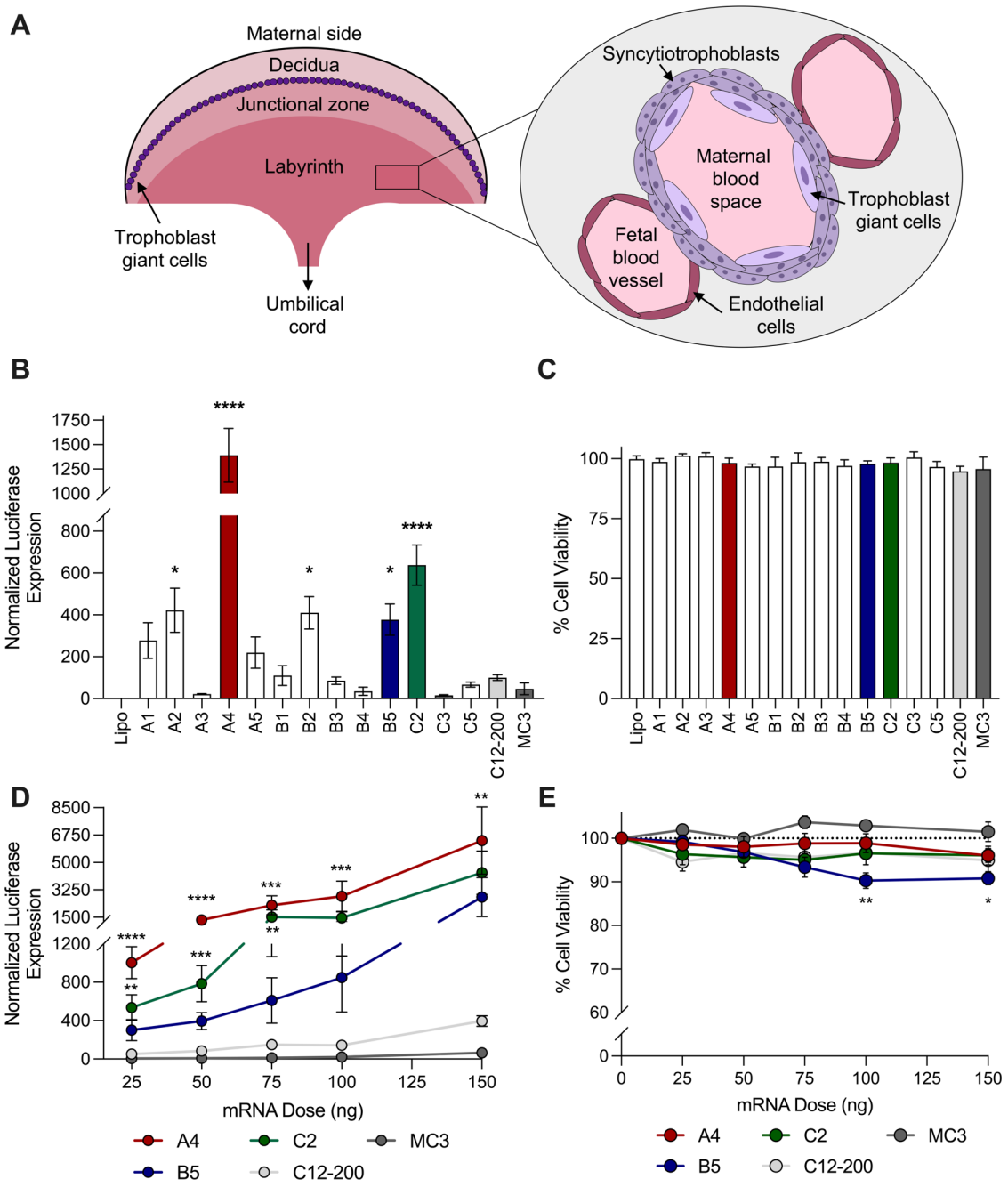

Figure 2. *In vitro* LNP-mediated luciferase mRNA delivery to placental cells. (A) Left: regions of the mouse placenta from the maternal to fetal side. Right: cell types separating the maternal and fetal blood spaces in the labyrinth region. (B, C) JEG-3 trophoblast cells were treated with LNPs or Lipofectamine MessengerMAX at a dose of 50 ng of luciferase mRNA per 25,000 cells for 24 h. Normalized luciferase expression was quantified by subtracting bioluminescence values from untreated cells and normalizing to the Lipofectamine group. Normalized luciferase expression is reported as mean ± SEM of $n = 6$ biological replicates (averaged from $n = 5$ technical replicates each). Percent cell viability for each treatment condition was normalized to untreated cells and is reported as mean ± SEM of $n = 4$ biological replicates (averaged from $n = 4$ technical replicates each). Nested one-way ANOVAs with *post hoc* Student's *t* tests using the Holm−Šídák correction for multiple comparisons were used to compare the normalized luciferase expression or cell viability across treatment groups to Lipofectamine. (D, E) Luciferase expression and cell viability were evaluated in a dose-dependent manner at 25, 50, 75, 100, and 150 ng of luciferase mRNA per 25,000 cells. Normalized luciferase expression is reported as mean ± SEM of $n = 6$ biological replicates (averaged from $n = 5$ technical replicates each) and percent cell viability is reported as mean ± SEM of $n = 4$ biological replicates (averaged from $n = 3$ technical replicates each). Nested one-way ANOVAs with *post hoc* Student's *t* tests using the Holm−Šídák correction for multiple comparisons were used to compare normalized luciferase expression or cell viability across treatment groups to Lipofectamine at each dose. $^{*}p \leq 0.05$, $^{**}p \leq 0.01$, $^{***}p \leq 0.001$, $^{****}p \leq 0.0001$.

vascular endothelial growth factor (VEGF) or placental growth factor (PlGF) or downregulating soluble fms-like tyrosine kinase-1 (sFlt-1, the soluble version of VEGF receptor 1), which is overexpressed in pre-eclampsia.[21−25] Most of these therapies have used viral approaches; however, due to the challenges associated with permanent, off-target VEGF expression, these therapies have been administered locally to the placenta via an invasive intrauterine artery injection.

https://doi.org/10.1021/jacs.2c12893
J. Am. Chem. Soc. XXXX, XXX, XXX−XXX

Alternatively, nonviral platforms, such as mRNA LNPs, offer the opportunity for transient VEGF expression via a simpler injection route, such as intravenous administration. However, LNP-mediated mRNA delivery to the placenta has been minimally evaluated during pregnancy. Extensive preclinical work in nonpregnant mice has demonstrated potent LNP-mediated mRNA delivery primarily to the liver upon intravenous administration.[8,26] Interestingly, the placenta shares many physiological features with the liver including high blood flow and a fenestrated endothelium, suggesting the potential for LNP-mediated mRNA delivery to the placenta during pregnancy.[27−29] Thus, we hypothesized that engineered LNPs capable of mRNA delivery to extrahepatic organs may mediate delivery to the placenta due to the high blood flow to the placenta during pregnancy.

Here, we engineer ionizable LNPs for mRNA delivery to the placenta with applications in mediating placental vasodilation using VEGF mRNA. To this end, we formulated 15 luciferase mRNA LNPs from a library of ionizable lipids and screened *in vitro* mRNA delivery in placental cells. From this screen, LNP A4 mediated potent *in vitro* luciferase expression and was identified as a lead formulation. LNP A4 and a C12-200 LNP, an industry-standard ionizable LNP formulation, were evaluated for *in vivo* luciferase mRNA delivery in nonpregnant and pregnant mice. LNP A4 enabled extrahepatic mRNA delivery and potent luciferase expression in the placentas of pregnant mice, while C12-200 LNPs mediated mRNA delivery primarily to the liver with little luciferase expression in the placenta. Upon characterization of cellular mRNA LNP delivery, LNP A4 mediated *in vivo* mCherry expression in trophoblasts, endothelial cells, and immune cells in the placenta. When assessing functional delivery of a clinically relevant cargo such as VEGF mRNA, LNP A4 mediated local VEGF expression in the placenta and an increase in fetal blood vessel area with a better safety profile compared to C12-200 LNPs. Collectively, these results demonstrate the potential for an mRNA LNP platform to promote e vasodilation in the placenta to potentially aid in treating disorders during pregnancy.

2. RESULTS AND DISCUSSION

2.1. Design and Characterization of Ionizable Lipid LNP Library. To engineer LNPs for mRNA delivery to the placenta during pregnancy, we formulated a library of LNPs each with their own unique ionizable lipid. Specifically, a library of ionizable lipids was synthesized, as previously described, using a fast and simple S_N2 reaction setup, where one of three epoxide tails—A (C12), B (C14), or C (C16)—was reacted with one of five polyamine cores—1, 2, 3, 4, or 5 (Figure 1A,B).[9] Liquid chromatography−mass spectrometry (LC-MS) was used to confirm the molecular identity of each of these 15 lipids (Figure S1). Reactions for the C1 and C4 lipids did not produce stable products, and these lipids were consequently removed from the library.

Each of the remaining 13 ionizable lipids was combined with 1,2-dioleoyl-*sn*-glycero-3-phosphoethanolamine (DOPE), cholesterol, and lipid-anchored poly(ethylene glycol) (PEG) to formulate LNPs via chaotic mixing with an aqueous phase of luciferase mRNA in a microfluidic device (Figure 1C).[30] Each of these lipid excipients plays a key role in LNP formulation, intracellular uptake, and delivery. The ionizable lipid enables mRNA encapsulation and endosomal escape for potent intracellular delivery, the phospholipid DOPE promotes LNP membrane formation, cholesterol enhances membrane stability, and lipid-PEG limits rapid clearance and immune cell opsonization.[10,31,32] In addition to our library of 13 LNPs each with their own unique ionizable lipid, we formulated two control LNPs with ionizable lipids C12-200 and DLin-MC3-DMA, which serve as industry-standard lipids for comparison (Figure S2).[33]

Following formulation, we characterized the hydrodynamic size, polydispersity index (PDI), encapsulation efficiency, and pK_a of the LNP library (Figure 1D). Thirteen of the 15 LNPs were less than 120 nm in diameter and 14 of the 15 LNPs had PDIs less than 0.2. LNPs A5, B5, and C5 were the largest LNPs from each of their respective groups by epoxide tail length, suggesting that polyamine core 5—having the highest molecular weight of all of the evaluated cores—could increase the size of the LNP formulations. Ten of the 15 LNPs had mRNA encapsulation efficiencies greater than 85%; interestingly, these formulations primarily had ionizable lipids with C12 or C14 epoxide tails. Finally, we characterized LNP pK_a, or the pH at which the LNP is 50% protonated. LNP pK_a depends largely on the ionizable lipid component and a value <7.0 indicates the ability of the LNP to escape the acidic environment of the endosome following endocytosis.[31] In the endosome, LNPs become protonated causing their membrane lipids to fuse with the anionic lipids of the endosome and release their mRNA cargo into the cytosol.[31,32] pK_a values for the LNP library ranged from 5.12 to 7.45, indicating the ionizable nature of our LNPs for potent intracellular mRNA delivery.

2.2. *In Vitro* mRNA LNP Delivery to Placental Cells. Next, we sought to evaluate the *in vitro* mRNA transfection efficiency of our LNP library in placental cells. We chose JEG-3 cells—an immortalized human choriocarcinoma cell line—which are often used for *in vitro* models of placental trophoblasts.[34] While there are many differences between the mouse and human placenta, trophoblasts are one of the major cell types in the placenta of both species. In the mouse placenta, there are three distinct cell regions from the maternal to fetal side (Figure 2A). The first region is the decidua, which is a thick mucosal membrane that houses placental immune cells and regulates trophoblast invasion into the uterus.[20] The second region is the junctional zone, which is separated from the decidua by trophoblast giant cells (TGCs) and is responsible for the main endocrine functions of the placenta. Finally, the labyrinth is where the majority of nutrient and gas exchange occurs between maternal and fetal blood. Within the labyrinth, the maternal blood spaces are separated from fetal blood vessels by the syncytiotrophoblast layer and TGCs, as well as a layer of fetal endothelial cells. Both the syncytiotrophoblast and endothelial cells secrete proteins, such as vascular endothelial growth factor (VEGF), that mediate vascularization in the placenta and impact the efficiency of oxygen transport to the fetus.[35,36] Therefore, *in vitro* mRNA delivery was assessed in trophoblast cells for applications in mediating placental vasodilation.

LNPs or Lipofectamine MessengerMAX were used to treat JEG-3 cells with 50 ng of luciferase mRNA per 25,000 cells. Lipofectamine is often considered a gold standard transfection reagent for *in vitro* nucleic acid delivery.[37,38] Luciferase expression as a measure of functional mRNA delivery was evaluated in JEG-3 cells 24 h following treatment with LNPs or Lipofectamine. Five LNPs from the 15 LNP library had significantly higher luciferase expression than Lipofectamine

https://doi.org/10.1021/jacs.2c12893
J. Am. Chem. Soc. XXXX, XXX, XXX−XXX

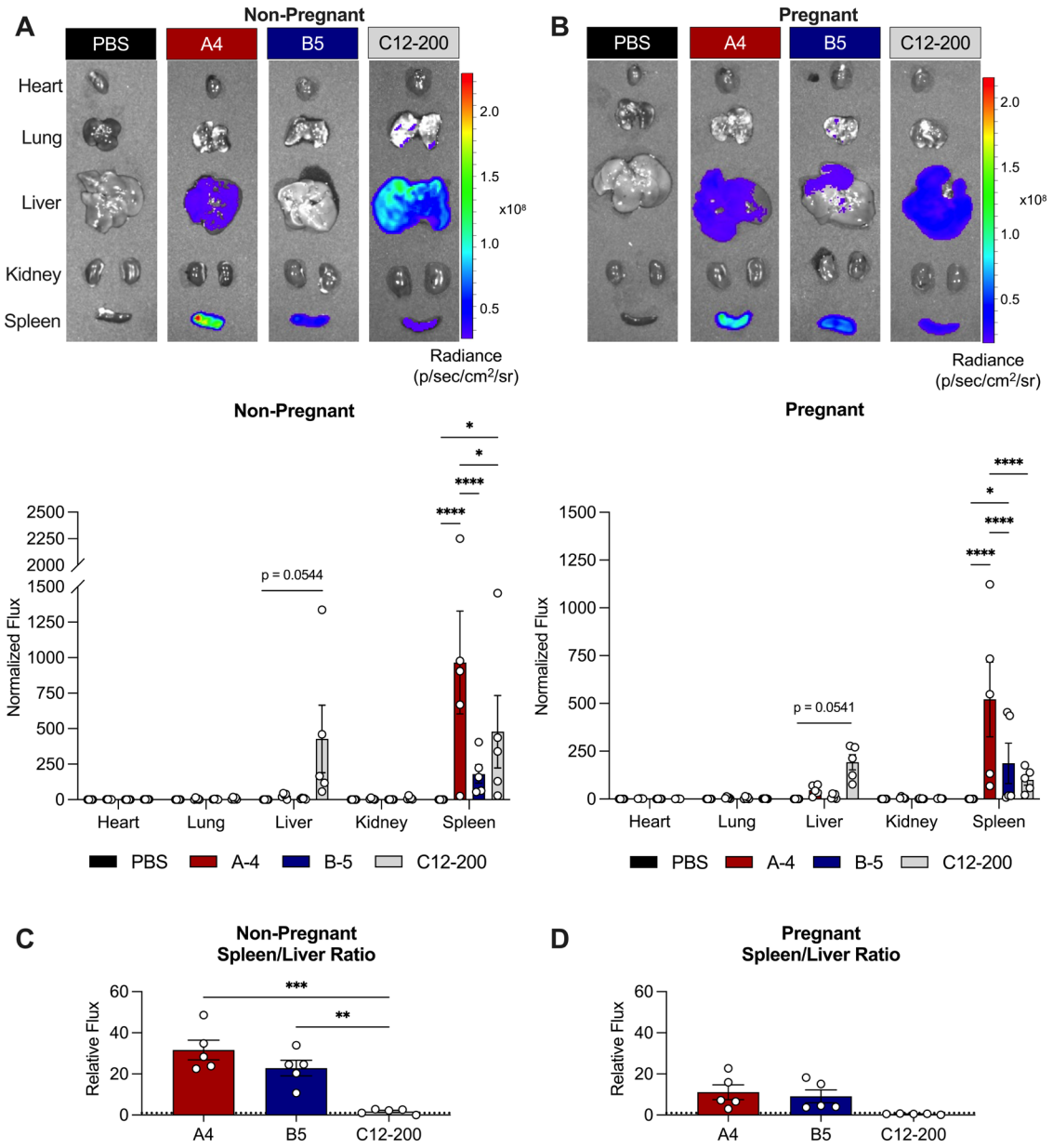

Figure 3. *In vivo* LNP-mediated luciferase mRNA delivery to the nonreproductive maternal organs of nonpregnant and pregnant mice. (A, B) IVIS images and quantification of luciferase mRNA LNP delivery (0.6 mg/kg) to the heart, lung, liver, kidneys, and spleen in (A) nonpregnant and (B) pregnant mice. For each treatment group, representative IVIS images are shown from the mouse with the normalized luminescence flux value in the spleen closest to the mean. Two-way ANOVAs with *post hoc* Student's *t* tests using the Holm−Šídák correction for multiple comparisons were used to compare normalized flux across treatment groups and organ. (C, D) Spleen-to-liver ratio for each LNP treatment group in (C) nonpregnant and (D) pregnant mice. One-way ANOVAs with *post hoc* Student's *t* tests using the Holm−Šídák correction for multiple comparisons were used to compare relative flux across treatment groups. All data are reported as mean ± SEM (n = 5 biological replicates). *$p \leq 0.05$, **$p \leq 0.01$, ***$p \leq 0.001$, ****$p \leq 0.0001$.

(Figure 2B). Of these top performers, two had the C12 epoxide tail, two had the C14 epoxide tail, and only one had the C16 epoxide tail. Additionally, only polyamine cores 2, 4, and 5 were represented among the top five performing LNPs. We also evaluated cell viability 24 h following treatment and none of the LNPs had a significant decrease in cell viability compared to Lipofectamine (Figure 2C).

We selected one optimal-performing LNP from each group by ionizable lipid epoxide length, and all three had a unique polyamine core: LNPs A4, B5, and C2. These LNPs, as well as the industry-standard C12-200 and MC3 LNPs, were used for *in vitro* dose-dependent evaluation of luciferase expression and cell viability (Figure 2D,E). The trends observed in the library screen at 50 ng of mRNA per 25,000 cells were also observed at both lower and higher doses. LNP A4 was selected as our lead candidate; LNP B5 with its average performance and the poor-performing C12-200 LNP were also selected for further evaluation. LNP C2 was not selected for *in vivo* evaluation due to its relatively poor mRNA encapsulation efficiency of 74%.

2.3. LNPs Mediate Greater Extrahepatic mRNA Delivery Than C12-200 LNPs in Nonpregnant and Pregnant Mice. LNPs A4, B5, and C12-200 were evaluated *in vivo* for luciferase expression in nonpregnant and pregnant mice. Previously, ionizable LNPs such as those utilizing the

https://doi.org/10.1021/jacs.2c12893
J. Am. Chem. Soc. XXXX, XXX, XXX−XXX

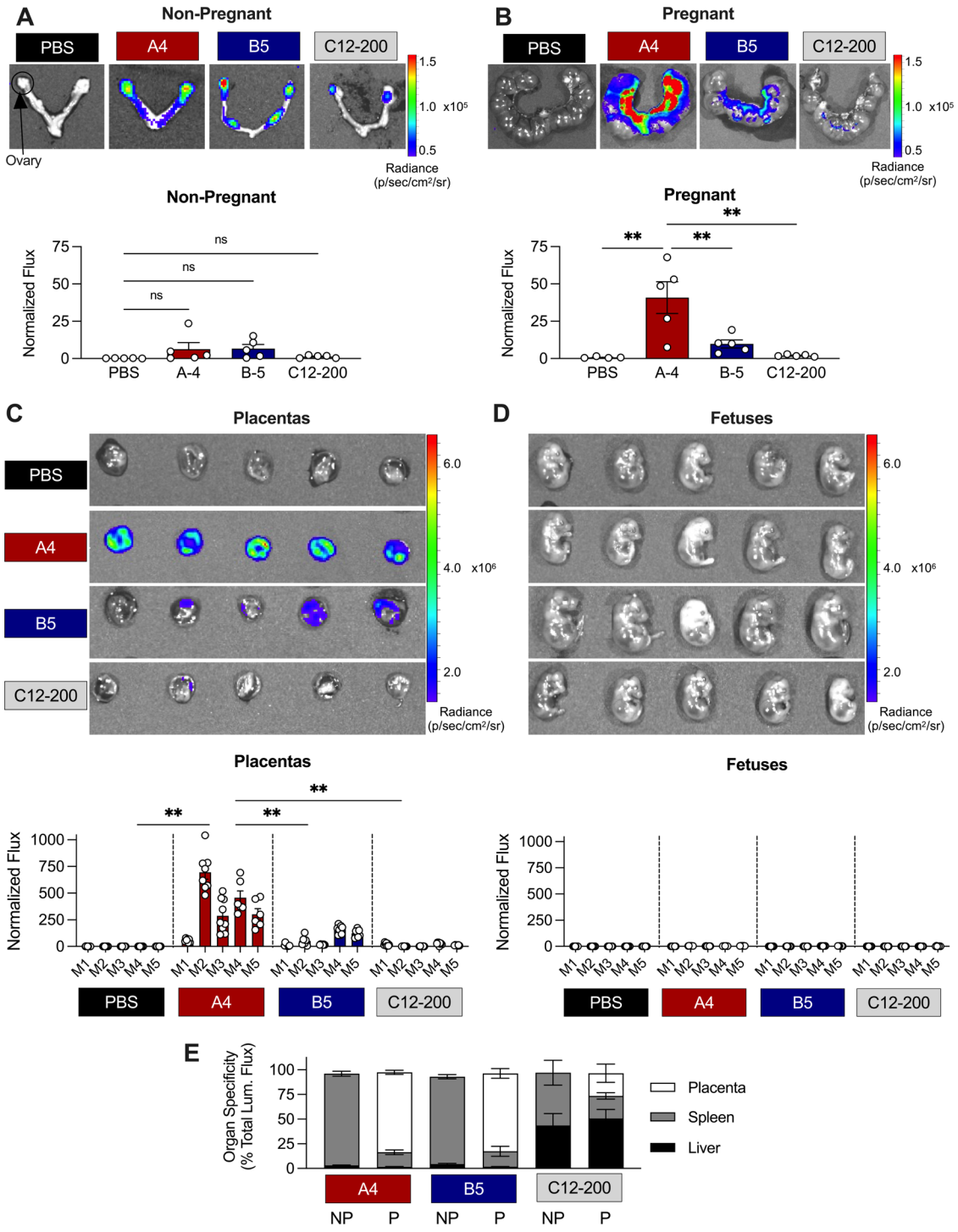

Figure 4. *In vivo* LNP-mediated luciferase mRNA delivery in nonpregnant and pregnant mice to the uterus, placentas, and fetuses. (A, B) IVIS images and quantification of luciferase mRNA LNP delivery (0.6 mg/kg) to the heart, lung, liver, kidneys, and spleen in (A) nonpregnant and (B) pregnant mice. Normalized flux in the uterus is reported as the mean ± SEM (n = 5 biological replicates). One-way ANOVAs with *post hoc* Student's t tests using the Holm−Šídák correction for multiple comparisons were used to compare normalized luminescence flux across treatment groups. (C, D) IVIS images and quantification of luciferase mRNA LNP delivery (0.6 mg/kg) to the placentas (C) and fetuses (D) of pregnant mice. Normalized flux in the fetuses and placentas are reported as the mean ± SEM for each mouse (n = 5 biological replicates each with n = 6−10 placentas and fetuses). Nested one-way ANOVAs with *post hoc* Student's t tests using the Holm−Šídák correction for multiple comparisons were used to compare normalized flux across treatment groups. For each treatment group, representative IVIS images are shown from the mouse with the normalized flux value in the uterus, placentas, or fetuses closest to the mean. (E) Organ specificity of each LNP treatment group calculated as a percent of total luminescent flux from the nonreproductive maternal organs, placentas, and fetuses. M: mouse, NP: nonpregnant, P: pregnant, $^{**}p \leq 0.01$.

C12-200 lipid have been shown to deliver mRNA predominantly to the liver upon intravenous administration due to the first-pass hepatic clearance effect and high blood flow in the liver.[8,9] However, we hypothesized that LNPs capable of

https://doi.org/10.1021/jacs.2c12893
J. Am. Chem. Soc. XXXX, XXX, XXX−XXX

delivering mRNA to extrahepatic organs upon intravenous administration may mediate delivery to the placenta based on the increased blood flow to the placenta during pregnancy. Therefore, we first assessed luciferase mRNA delivery to the nonreproductive maternal organs—heart, lung, liver, kidneys, and spleen—in nonpregnant and pregnant mice.

Nonpregnant and gestational day E16 pregnant mice were treated with PBS or LNPs at a dose of 0.6 mg/kg of luciferase mRNA via tail vein injection. Six hours later, mice were injected with luciferin, euthanized, and their nonreproductive organs were removed. An *in vivo* imaging system (IVIS) was used to measure and quantify luciferase expression in each of the organs using regions of interest (ROIs). In both nonpregnant and pregnant mice, C12-200 LNPs mediated greater delivery to the liver than LNPs A4 and B5 (Figures 3A,B, S3, and S4). Instead, with LNP A4 there was significantly higher delivery to the spleen than LNPs B5 and C12-200 in both nonpregnant and pregnant mice. These results suggest the ability of LNP A4 to deliver mRNA to extrahepatic organs such as the spleen.

One possible explanation for these extrahepatic delivery results is the design of the ionizable lipid structures. Unlike the C12-200 ionizable lipid, the A4 lipid structure includes oxygen atoms in the form of ester linkages that contribute to the overall electronegativity of the molecule. Other works have observed that either oxygen-containing or negatively charged lipids have also mediated extrahepatic delivery to the spleen.[11,39] Future work might involve pooled high-throughput screening methodologies to enable a more robust analysis of structure−function relationships and address the often weak correlation observed between *in vitro* and *in vivo* delivery.[40]

LNP size differences could also play a role, as discussed by Chen et al., who suggest that larger LNPs might be unable to penetrate the 100−140 nm fenestrations in liver vasculature, therefore limiting LNP biodistribution in the liver.[41] However, LNP A4 (93.44 ± 1.18 nm) and the C12-200 LNP (82.11 ± 3.28 nm) are very similar in size and are both below the size cutoff of mouse liver fenestrations, yet the C12-200 LNP mediates more substantial liver delivery in both pregnant and nonpregnant mice.

There were no significant differences in the normalized luciferase expression values between nonpregnant and pregnant mice for the nonreproductive organs across all treatment groups (Figure S6A−E). However, we sought to further evaluate the differences in extrahepatic delivery between nonpregnant and pregnant mice. To do so, we divided the bioluminescent flux measurements from the spleen by the liver measurements to calculate a spleen-to-liver ratio for all of the LNP treatment conditions. In nonpregnant mice, LNPs A4 and B5 had significantly higher spleen/liver ratios than C12-200, demonstrating that these formulations enabled greater spleen than liver delivery (Figure 3C). Interestingly, the spleen/liver ratios for LNPs A4 and B5 were significantly higher in nonpregnant mice than pregnant mice, suggesting less relative spleen delivery during pregnancy when compared to liver delivery (Figures 3D and S6G).

It is possible that these differences in the spleen/liver ratio between nonpregnant and pregnant mice could be explained by the first-pass hepatic clearance effect, where LNPs that are able to escape delivery to the liver can deliver to extrahepatic organs such as the spleen. Pregnancy essentially introduces a new extrahepatic organ—the placenta—with high blood flow demands. Therefore, the lower spleen/liver ratio in pregnant mice could potentially be explained by the partitioning of extrahepatic mRNA delivery between the spleen and placenta.

We next evaluated mRNA LNP-mediated luciferase expression to the uterus and ovaries in both nonpregnant and pregnant mice. Upon imaging, there appeared to be luciferase expression in both the uterus and ovaries of LNP-treated nonpregnant mice; however, the quantified bioluminescent flux values were very low compared to the other organs of interest, and delivery for the LNP treatment groups was not significant compared to PBS (Figures 4A, S3, and S4). In the case of pregnant mice, the uterus was dissected from the mouse and imaged intact, with the fetuses and placentas still inside. We observed significant luciferase expression in the uterus of the LNP A4-treated group compared to PBS (Figure 4B). For LNP A4, the normalized luciferase expression in the uterus was significantly higher in pregnant mice than nonpregnant mice (Figure S6F). These results suggest that the increased blood flow to the uterus during pregnancy to supply oxygen and nutrients to the fetus and placenta could play a role in impacting the biodistribution of LNP A4.

2.4. Potent LNP-Mediated mRNA Delivery to the Placenta in Pregnant Mice. Then, we proceeded to dissect the uterus from pregnant mice to remove and image the placentas and fetuses. For the LNP A4 treatment group, there was significant bioluminescent flux in the placentas compared to the PBS-treated placentas (Figures 4C and S5). In agreement with our *in vitro* results, where LNP A4 was our lead candidate, this LNP mediated significantly higher *in vivo* luciferase mRNA delivery to the placenta compared to LNPs B5 and C12-200. There was no luciferase expression in the fetuses for any of the LNP treatment groups, suggesting the safety of this LNP platform for mRNA delivery to the placenta (Figures 4D and S5).

While this is, to the best of our knowledge, one of the first studies to evaluate mRNA LNP delivery in pregnant mice, there are numerous studies that evaluate the *in vivo* biodistribution of other nanoparticle platforms to the placentas and fetuses.[42−46] Some of these works explore the effect of nanoparticle size on placental transport, including a study that observed localization in the fetus for 1.4 and 18 nm gold nanoparticles, but not for 80 nm gold nanoparticles.[42] This is consistent with our results using 80−120 nm LNPs, where we observed no placental transport and luciferase expression in the fetus. Besides the various tight junctions regulating placental transport, it has been hypothesized that this size-dependent effect is due to the presence of transtrophoblastic channels, which are ∼20 nm in diameter and separate maternal and fetal circulation.[42,47,48] Based on this hypothesis, many nanoparticle platforms, such as those employed here, would be unable to utilize these channels to enter fetal circulation due to their size.

We also sought to evaluate the organ specificity of each mRNA LNP treatment in both nonpregnant and pregnant mice. To do this, we totaled luminescent flux measurements from the nonreproductive maternal organs, placentas, and fetuses (if applicable) and calculated the percent of total luminescent flux for each organ (Figure 4E). Interestingly, the percent liver delivery remained about the same between nonpregnant and pregnant mice for all three LNP formulations. For LNPs A4 and B5, less than 4% and 5%, respectively, of total luminescent flux were from the liver, indicating the extrahepatic specificity of these LNPs. Instead, with the C12-200 formulation, between 44% and 51% of the total luminescent flux was from the liver. When we compared

https://doi.org/10.1021/jacs.2c12893
J. Am. Chem. Soc. XXXX, XXX, XXX−XXX

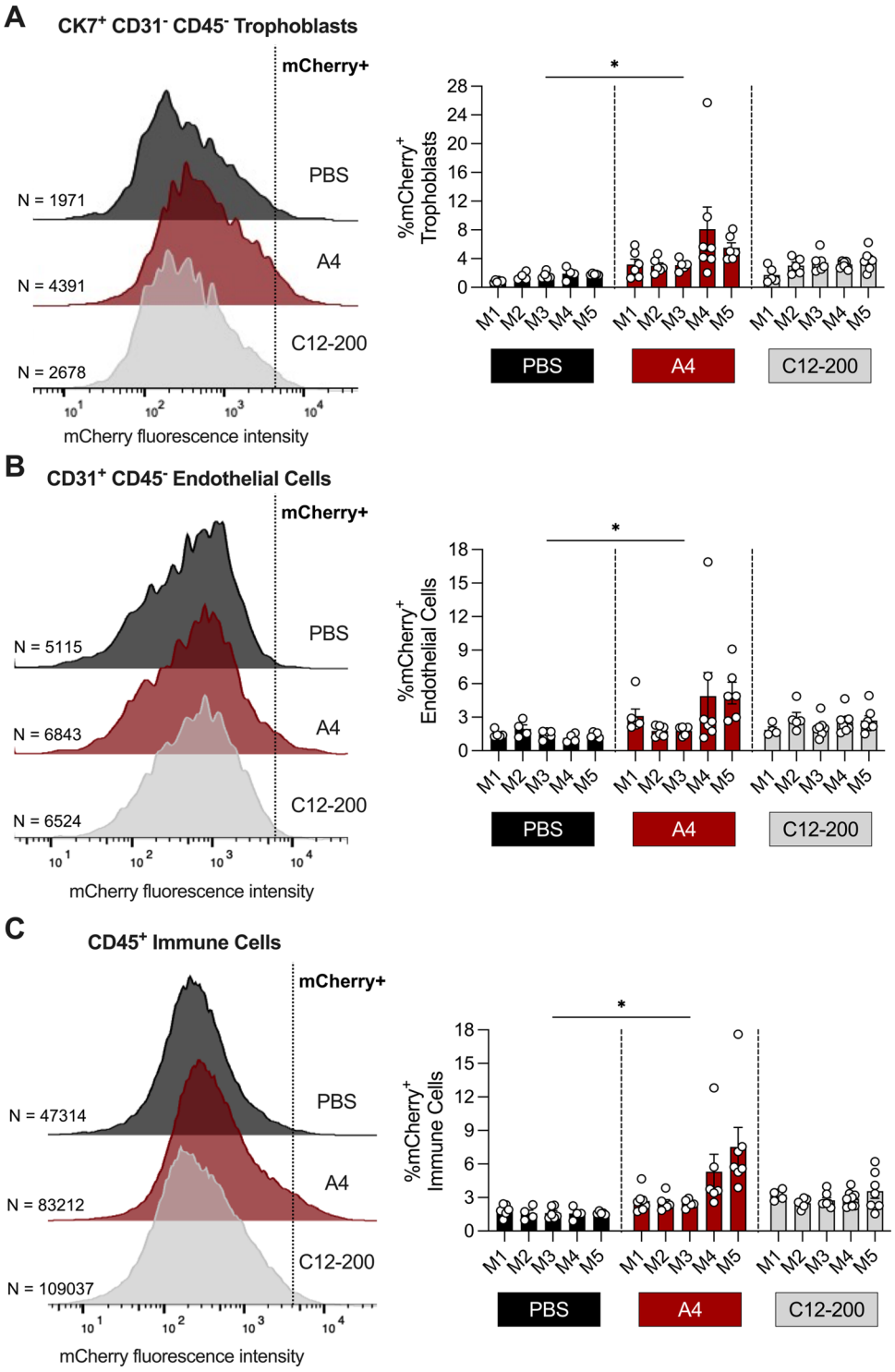

Figure 5. Characterizing *in vivo* LNP-mediated mCherry mRNA delivery to the placentas in pregnant mice. (A–C) Pregnant mice were treated with mCherry mRNA LNPs at a dose of 1 mg/kg and placentas were collected 12 h later for flow cytometry analysis. Histograms and quantification of percent mCherry$^+$ cells in (A) cytokeratin-7$^+$ (CK7) CD31$^-$CD45$^-$ trophoblasts, (B) CD31$^+$CD45$^-$ endothelial cells, and (C) CD45$^+$ immune cells in the placenta. Percent mCherry$^+$ cells are reported as the mean ± SEM for each mouse (n = 5 biological replicates each with n = 4–8 placentas). Nested one-way ANOVAs with *post hoc* Student's t tests using the Holm–Šídák correction for multiple comparisons were used to compare percent mCherry$^+$ cells across treatment groups. For each treatment group, representative histograms with their respective cell counts are shown from the mouse with the value for percent mCherry$^+$ cells closest to the mean. M: mouse, *$p \leq 0.05$.

nonpregnant and pregnant mice, the only extrahepatic delivery for nonpregnant mice was observed in the spleen, which then becomes partitioned between the spleen and placenta in pregnant mice. For LNP A4, about 81% of the total luminescent flux was from placental delivery in comparison to 79% for LNP B5 and 23% for C12-200. With both the highest magnitude of delivery and the highest specificity to the

https://doi.org/10.1021/jacs.2c12893
J. Am. Chem. Soc. XXXX, XXX, XXX–XXX

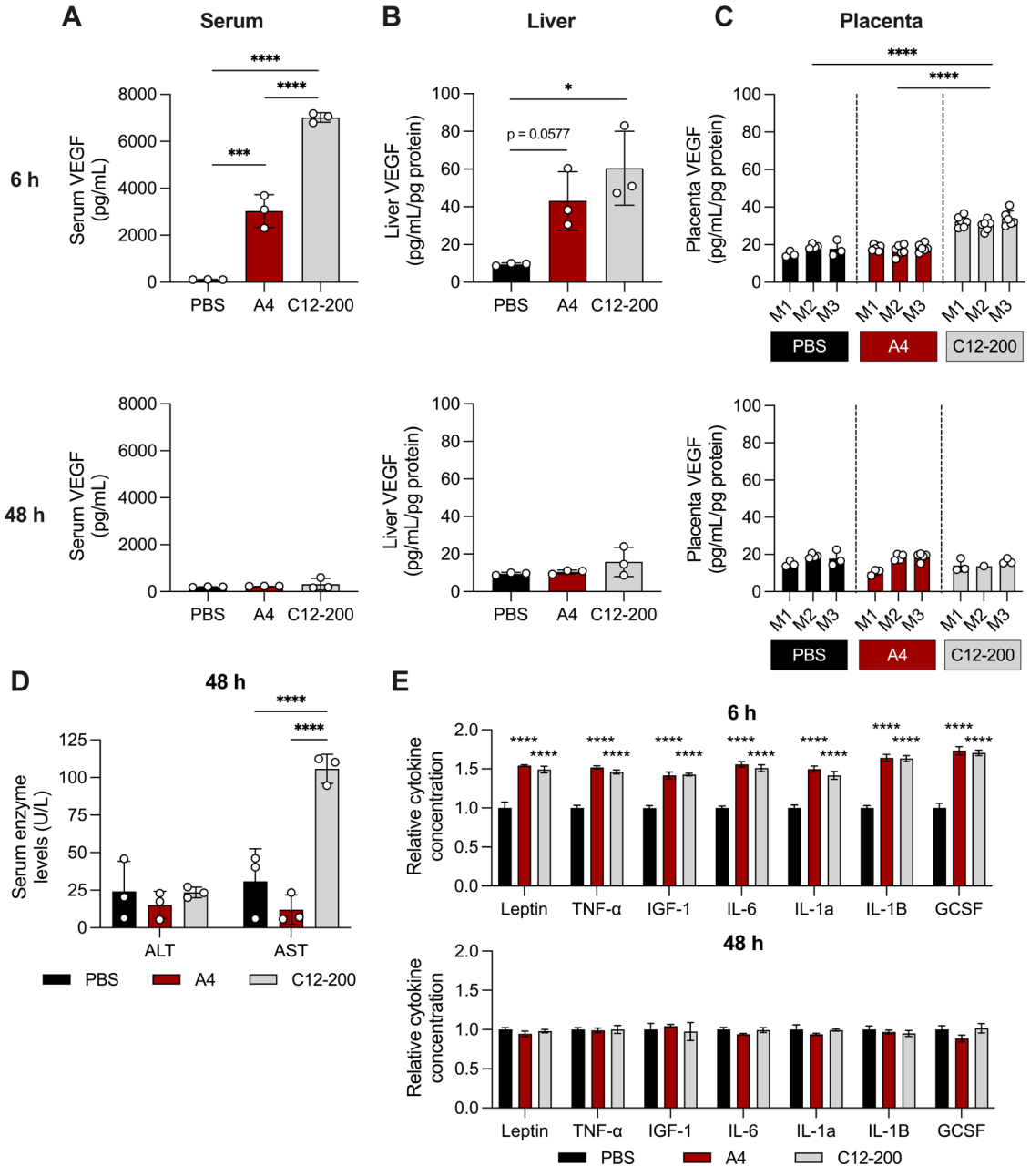

Figure 6. Evaluation of VEGF expression and toxicity in pregnant mice treated with VEGF mRNA LNPs. (A–C) VEGF expression in (A) serum, (B) livers, and (C) placentas from pregnant mice both 6 h and 48 h following treatment with PBS or VEGF mRNA LNPs at a dose of 1 mg/kg. VEGF concentration in livers and placentas was normalized to the mass of total protein in the tissue homogenate. For serum and livers, VEGF concentration is reported as mean ± SD (n = 3 biological replicates) and for placentas, VEGF concentration is reported as the mean ± SD for each mouse (n = 3 biological replicates each with n = 4–8 placentas). For serum and livers, one-way ANOVAs with *post hoc* Student's t tests using the Holm–Šídák correction for multiple comparisons were used to compare the VEGF concentration across treatment groups. For placentas, nested one-way ANOVAs with *post hoc* Student's t tests using the Holm–Šídák correction for multiple comparisons were used to compare the VEGF concentration across treatment groups. (D) ALT and AST enzyme levels in serum 48 h after treatment with PBS or VEGF mRNA LNPs. A two-way ANOVA was performed on serum enzyme levels with *post hoc* Student's t tests using the Holm–Šídák correction for multiple comparisons. Data are reported as mean ± SD (n = 3 biological replicates). (E) Cytokine levels in placental tissue homogenates both 6 and 48 h following treatment with PBS or VEGF mRNA LNPs. For each cytokine, data are normalized to the average of the optical density measurements for the PBS-treated mice. Data are reported as mean ± SD (n = 3 biological replicates). M: mouse, *$p \leq 0.05$, ***$p \leq 0.001$, ****$p \leq 0.0001$.

placenta, LNP A4 was shown to be the lead candidate for placental mRNA delivery.

While it has been shown that benchmark LNPs—such as those containing the C12-200 or DLin-MC3-DMA ionizable lipids—deliver mRNA primarily to the liver, there are several cardiovascular changes that occur during pregnancy that we sought to exploit for selective mRNA delivery to the placenta. By 24 weeks of gestation in human pregnancy, there is a 45% increase in total cardiac output compared to nonpregnant individuals.[49] 20–25% of this cardiac output represents blood flow to the uterus and placenta, while blood flow to the liver as a function of cardiac output is lower during pregnancy compared to nonpregnant individuals.[50] Due to these effects, we hypothesized that LNPs capable of delivering mRNA to

https://doi.org/10.1021/jacs.2c12893
J. Am. Chem. Soc. XXXX, XXX, XXX–XXX

extrahepatic organs in nonpregnant mice might be able to deliver mRNA to the placenta in pregnant mice. Interestingly, we saw that LNP A4 was capable of extrahepatic luciferase mRNA delivery to the spleen in nonpregnant mice which was then partitioned between the spleen and placenta in pregnant mice. With 81% of the total luminescent flux originating from the placenta, LNP A4 demonstrated not only placental specificity but also the highest magnitude of luciferase expression of the three LNP formulations evaluated.

2.5. Characterizing *In Vivo* LNP mRNA Delivery to Placental Cells. We proceeded to further evaluate LNP A4 as our lead candidate for placental delivery and the C12-200 LNP as an industry-standard control. In addition to demonstrating luciferase mRNA delivery to the placenta, we used these LNPs to encapsulate mCherry mRNA for *in vivo* cellular level characterization of mRNA delivery to the mouse placenta. Twelve hours after PBS or LNP administration in pregnant mice, cells were isolated from dissected placentas and stained for trophoblasts using the intracellular pan-trophoblast marker cytokeratin-7 ($CK7^+CD31^-CD45^-$), endothelial cells ($CD31^+CD45^-$), and immune cells ($CD45^+$)[51,52] (Figure S7). LNP A4 mediated significant *in vivo* mCherry mRNA delivery to trophoblasts, endothelial cells, and immune cells in the placenta compared to the PBS-treated group (Figure 5A–C). 4.58% of trophoblasts were $mCherry^+$ in the LNP A4-treated group compared to 3.02% and 1.57% in the C12-200 and PBS groups, respectively (Figure 5A). In endothelial cells, the mCherry positivity rates were 1.45%, 3.34%, and 2.44% for the PBS, LNP A4, and C12-200 LNP treatment groups, respectively (Figure 5B). Finally, 4.11% of immune cells from the LNP A4 group were $mCherry^+$ compared to 2.99% and 1.68% in the C12-200 LNP and PBS groups (Figure 5C). Overall, these results with mCherry mRNA follow the same general trend we observed with luciferase mRNA, where LNP A4 demonstrated higher mRNA delivery to the placenta. These results suggest the ability of our LNPs to deliver to the two major cell types of the placenta, trophoblasts and endothelial cells, which are also the target cells for treating placental insufficiency disorders. Additionally, placental immune cells are believed to play a role in pregnancy disorders, such as FGR, and could be a novel target for treating these conditions.[53]

To our knowledge, this is one of the first such works to deliver mRNA therapeutics to various cell populations in the placenta during pregnancy. As a result, it is difficult to comment on the clinical significance of ~3% to 5% $mCherry^+$ trophoblasts, endothelial cells, and immune cells in the placenta. However, we can make comparisons to other works that have delivered mRNA LNPs to extrahepatic organs, such as the spleen and lymph nodes, and characterized cellular level delivery.[10,11,54] Kheirolomoom et al. developed a CD3-targeting LNP platform encapsulating mCherry mRNA and observed positivity rates in splenic immune cells ranging from ~1.5% to 4%.[54] Fenton et al. utilized fluorescently labeled mRNA and demonstrated splenic immune cell association positivity rates ranging from ~2% to 6%.[11] However, with Cy5-labeled mRNA, fluorescence detection is indicative of mRNA accumulation or association in a particular cell type, rather than the functional protein expression. Third, Oberli et al. commented on the challenges of characterizing *in vivo* delivery of mRNA encoding fluorescent proteins and instead used genetically engineered Ai14D reporter mice for the delivery of Cre recombinase-encoding mRNA.[10] Using this model, the group demonstrated delivery to about 1–5% of immune cells in the lymph nodes. It is accepted in the field that positivity rates are substantially higher for Cre mRNA-mediated recombination than when delivering fluorescent protein encoding mRNA. A single copy of Cre-recombinase can mediate excision of a stop cassette and result in detectable signal, whereas multiple copies of mCherry or GFP protein are typically required to detect signal. Together, we believe that our positivity rates of 3–5% in trophoblasts, endothelial cells, and immune cells in the placenta signify successful mRNA delivery.

2.6. mRNA LNPs Mediate VEGF Expression with Minimal Toxicity *In Vivo*. We next sought to evaluate the functional delivery of a clinically relevant mRNA for placental disorders using LNP A4 and the industry-standard C12-200 LNP. Specifically, we chose vascular endothelial growth factor (mouse isoform $VEGF_{164}$-A) mRNA, as both recombinant VEGF protein and adenovirus-mediated gene therapies have been explored for placental disorders, such as pre-eclampsia and fetal growth restriction.[21−24,55] Additionally, a VEGF-A mRNA therapeutic (AZD8601) is currently being evaluated in clinical trials by Moderna Inc. and AstraZeneca for patients with heart failure undergoing coronary artery bypass grafting.[56,57] Physiologically, VEGF-A binds and activates both VEGF receptor 1 (VEGFR1) and VEGF receptor 2 (VEGFR2), which are present on both trophoblasts and endothelial cells in the placenta, to regulate angiogenesis and vasodilation.[21,58,59]

To this end, healthy, gestational age E16 pregnant mice were treated with either PBS or VEGF mRNA LNPs. 6 and 48 h following LNP administration, VEGF expression was evaluated in serum, livers, and placentas. 6 h following LNP treatment, serum levels of VEGF for both LNP A4 and C12-200 were significantly elevated compared to PBS, with significantly higher VEGF levels for the C12-200 LNP group than LNP A4 (Figure 6A). At 48 h, serum levels for both LNP treatment groups returned to baseline, demonstrating the transient nature of VEGF mRNA therapy. These results in the serum are encouraging, particularly for a systemically administered therapeutic. Swanson et al. have previously utilized an adenovirus vector encoding VEGF-A for local administration to the uterine arteries in a guinea pig model of FGR.[23] With this platform, they observed VEGF concentration in maternal serum to be ~100 pg/mL to 200 pg/mL, which is up to 10-fold lower than our results with VEGF-A mRNA LNPs.

At 6 h, only the C12-200 LNP mediated significant VEGF expression in the liver (Figure 6B). At 48 h, VEGF expression in the liver also returned to baseline. In the placenta 6 h after LNP administration, there was significant VEGF expression for the C12-200 LNP-treated mice compared to the LNP A4 and PBS groups (Figure 6C). At 48 h, the VEGF levels in the placenta were at baseline for all groups. Negative control LNPs, encapsulating mCherry mRNA, were also used to evaluate the effect of A4 and C12-200 LNPs themselves on VEGF levels. Six hours following administration, there were no significant differences in serum or liver VEGF levels for the LNP treatment groups compared to the PBS control, suggesting minimal effect of the LNP carrier on VEGF expression (Figure S8).

As expected, the C12-200 LNP mediated higher serum levels of VEGF than the A4 LNP, consistent with the high luciferase mRNA expression in the liver with C12-200 LNPs and the efficacy of protein production by hepatocytes. In addition to measuring the serum levels of VEGF, a metric commonly used

https://doi.org/10.1021/jacs.2c12893
J. Am. Chem. Soc. XXXX, XXX, XXX−XXX

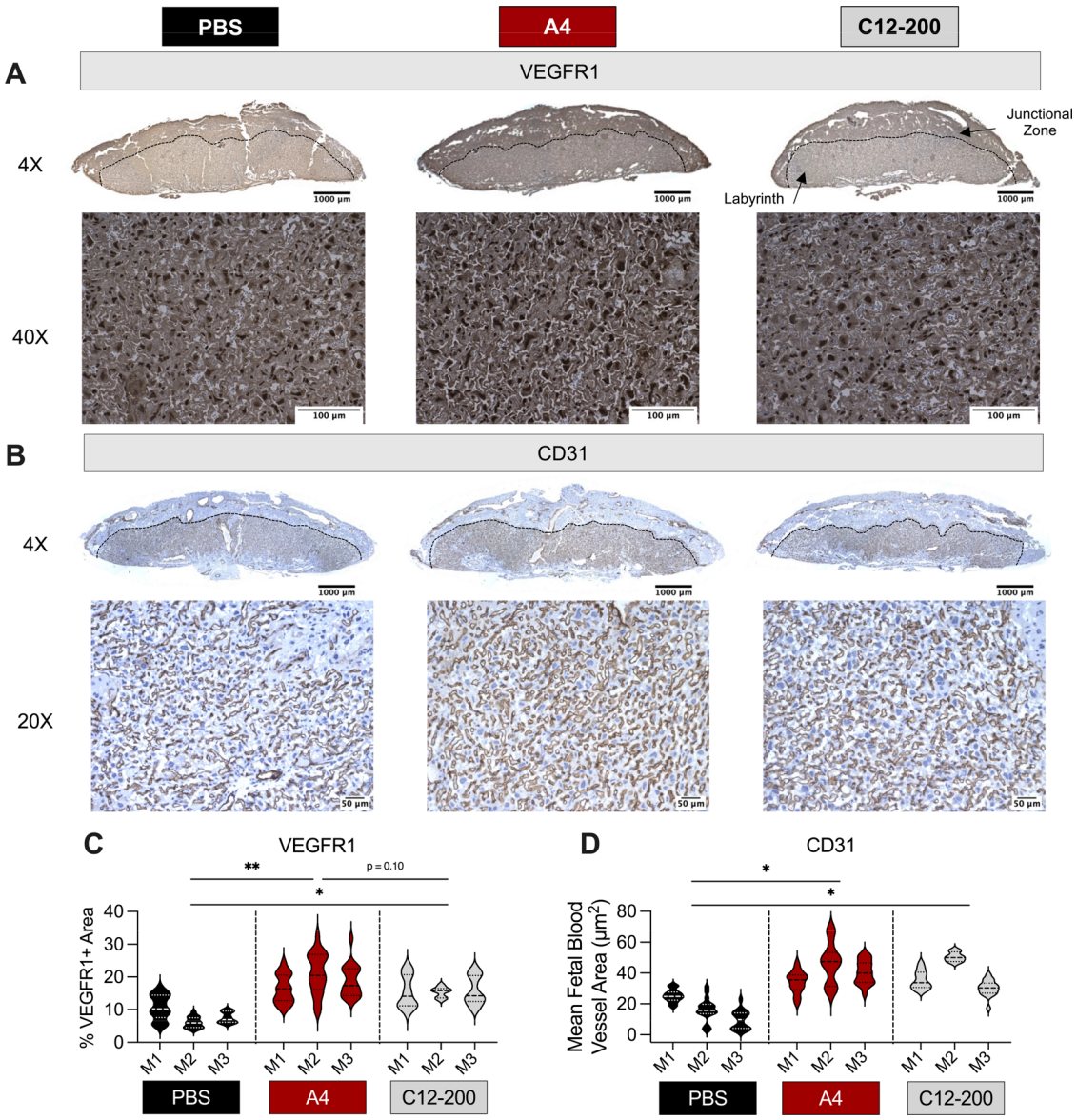

Figure 7. Assessing local VEGF expression and vasodilation in the placenta after treating pregnant mice with VEGF mRNA LNPs. (A) 4× and 40× images from VEGFR1 stained placentas. In the 4× images, the junctional zone and labyrinth are divided by a dashed black line. In the 40× images, the brown VEGFR1 staining is darker in the LNP A4 group, particularly in the regions surrounding the white blood spaces. (B) 4× and 20× images from CD31 stained placentas. Regions positive for CD31 are stained brown and denote fetal blood spaces. For VEGFR1 and CD31 staining, representative images are shown for each treatment group that had percent positive VEGFR1 positive area or mean fetal blood vessel area measurements closest to the mean. (C) Quantification of percent VEGFR1 positive area from VEGFR1 stained placentas using ImageJ. (D) Quantification of fetal blood vessel area from CD31 stained placentas using ImageJ. Nested one-way ANOVAs with *post hoc* Student's *t* tests using the Holm−Šídák correction for multiple comparisons were used to compare percent VEGFR1 positive area or mean fetal blood vessel area across treatment groups. Data are reported as median with first and third quartiles (n = 3 biological replicates with n = 3 placentas per mouse, n = 2 sections per placenta, and n = 3 distinct images per section for a total of n = 54 images per treatment group). M: mouse, $*p \leq 0.05$, $**p \leq 0.01$.

by the field to indicate functional mRNA delivery, we sought to further explore liver and placental levels of VEGF.[9,60,61] Liver VEGF levels followed similar trends as those observed in the serum. However, in the placenta, there was no measured difference in VEGF levels between the LNP A4 and PBS groups at 6 h. We think that these results are due to the rapid secretion of VEGF by placental cells into the surrounding tissue and serum and also the protein's relatively short half-life (about 15−30 min).[62,63]

Next, we assessed LNP-mediated liver toxicity by measuring serum levels of the secreted liver enzymes alanine aminotransferase (ALT) and aspartate aminotransferase (AST). These enzymes are often used to assess nanoparticle-mediated toxicity, as elevated levels of either enzyme can indicate hepatic injury due to high nanoparticle accumulation in the liver.[60,64] Forty-eight hours after LNP administration, there were no significant changes in ALT levels compared to PBS for either of the LNP treatment groups (Figure 6D). However, C12-200 LNPs resulted in significantly higher AST levels compared to PBS (3.5-fold) and LNP A4 (8.7-fold), perhaps suggesting some liver toxicity of the C12-200 LNPs. These results correlate with the high luciferase and VEGF expression in the liver for mice treated with C12-200 LNPs and demonstrate the

https://doi.org/10.1021/jacs.2c12893
J. Am. Chem. Soc. XXXX, XXX, XXX−XXX

benefit of delivery platforms, such as LNP A4, which have increased specificity to the placenta.

We also assessed LNP-mediated inflammation in the placenta at both 6 h and 48 h following LNP administration. Ensuring that our LNP platform induces minimal inflammation and immune system activation in the placenta is critical for translating the therapy to treat disorders such as pre-eclampsia, as pre-existing inflammation in the placenta is a key marker of the disorder.[65] To this end, we selected seven cytokines that have been shown to mediate inflammation in the placenta and assessed the relative concentration of each cytokine in LNP-treated mice compared to PBS-treated mice.[65,66] As is typically observed at acute timepoints following LNP administration, at 6 h, the relative cytokine concentrations were elevated for the LNP treatment groups compared to the PBS control (Figure 6E). By 48 h following administration, the elevated cytokine levels resolved and there were no significant increases in the relative concentrations of any of the seven cytokines between the LNP and PBS-treated groups. These results highlight the safety of LNPs for mRNA delivery to the placenta with minimal long-term effects on placental inflammation.

2.7. VEGF mRNA LNPs Mediate Vasodilation in the Placenta. To supplement the ELISA–based detection of VEGF expression, we utilized immunohistochemical (IHC) staining for VEGFR1 and VEGFR2 in the placenta, a technique utilized by other groups following intrauterine artery administration of adenovirus vectors encoding VEGF-A for placental vasodilation.[22,23] In these studies, positive VEGFR1 and VEGFR2 staining was used to indicate receptor upregulation in response to a local increase in VEGF-A expression.

Placentas were collected from pregnant mice 48 h following treatment with PBS, LNP A4, or C12-200 LNP and stained for VEGFR1 using chromogenic detection with horseradish peroxidase so that positively stained regions appear brown. Using a 4× objective to capture an image of the entire placental section, there is an obvious increase in VEGFR1 expression for the LNP A4-treated group (Figure 7A). Next, a 40× objective was used to capture images in the labyrinth region, where white regions depict blood vessel spaces (both maternal and fetal). For the LNP A4 treatment group, increased VEGFR1 expression is evident in the dark brown regions surrounding the white blood vessel areas in the 40× images. ImageJ was used to quantify the percent VEGFR1 positive area for each image taken within the labyrinth region. The percent VEGFR1 positive area significantly increased for the LNP A4 and C12-200 treatment group compared to the PBS control (Figure 7C). While the difference in percent VEGFR1 positive area between the LNP A4 and C12-200 treatment groups was not significant ($p = 0.10$), these results are encouraging, especially given the superior safety profile of LNP A4. C12-200 LNPs increased the serum levels of the secreted AST liver enzyme by about 3.5-fold compared to PBS, suggesting some nanoparticle-mediated toxicity due to high accumulation in the liver. These results would likely limit the clinical translation of C12-200 LNPs for placental insufficiency disorders, as repeat dosing would be essential for LNP-mediated protein replacement therapy in this application.

We also performed IHC for VEGFR2 expression and observed a slight increase in positive staining for the LNP A4 treatment group compared to PBS-treated mice (Figure S9). However, staining for VEGFR2 was substantially weaker than for VEGFR1; therefore, ImageJ quantification was not performed.

These results, along with the VEGF levels in serum, indicate that both systemic and local VEGF mRNA delivery are likely to play a role in placental VEGF expression. For example, if systemic VEGF mRNA delivery was solely responsible for VEGFR1 expression in the placenta, we would expect to see a roughly 2-fold increase in VEGFR1 expression for the C12-200 LNP treatment group compared to LNP A4, correlating with the 2-fold higher serum VEGF levels for the C12-200 LNP. However, local VEGF mRNA delivery is also playing a role as VEGFR1 expression in the placenta is visibly stronger in the labyrinth for the LNP A4 treatment group (Figure 7A). Also, while the difference in VEGFR1 quantification for the LNP A4 group was not significantly higher ($p = 0.10$) than the C12-200 LNP, these results are encouraging, especially given the better safety profile of LNP A4 (Figures 6D and 7C).

In addition to assessing local VEGF expression, we evaluated functional VEGF-mediated vasodilation in the placenta 48 h after LNP treatment. First, placentas were stained with hematoxylin and eosin (H&E) and imaged using 40× objectives. Images taken in the labyrinth region depict blood vessel spaces (both maternal and fetal) as white regions filled with red blood cells. Large purple-stained nuclei represent trophoblasts, while small purple-stained nuclei are fetal endothelial cells. Compared to PBS-treated mice, there is a visible increase in the blood vessel area for both LNP A4 and C12-200 treated placentas (Figure S10). Interestingly, for the LNP A4 group, the increase in blood vessel area appears more homogeneous, while for mice treated with C12-200 LNPs, some blood vessels are excessively dilated, and others are unaffected. We hypothesized that these differences might be due to the local versus systemic expression of VEGF for the A4 and C12-200 LNPs, respectively.

Finally, we used IHC to stain placental sections for CD31. As an endothelial cell marker, CD31-stained regions denote fetal blood spaces in the labyrinth region of the placenta[67,68] (Figure 2A). Images taken with a 4× objective clearly show the divide between the junctional zone and the labyrinth (Figure 7B). The junctional zone has very few endothelial cells (primarily only those that line maternal vessels and arteries supplying blood to the placenta), while the villi in the labyrinth region are rich in fetal endothelial cells to mediate oxygen and nutrient transport between maternal and fetal circulation.

Images of CD31 stained placentas taken in the labyrinth region at 20× demonstrate an increased intensity of CD31 staining for the LNP A4 treatment group compared to PBS-treated placentas (Figure 7B). We used the particle analysis tool in ImageJ to quantify fetal blood vessel area from CD31-stained placental sections. Mean fetal blood vessel area was significantly increased for the LNP A4 and C12-200 treatment groups compared to the PBS control (Figure 7D). These results suggest VEGF mRNA LNP-mediated functional vasodilation in the placenta as a promising therapeutic for placental disorders.

3. CONCLUSIONS

In summary, we developed an ionizable LNP platform for mRNA delivery to the placenta with applications in mediating placental vasodilation using VEGF mRNA. Our lead candidate LNP A4, identified for its potent *in vitro* mRNA delivery in placental cells, enabled high luciferase mRNA delivery to the placenta in pregnant mice. This LNP platform was also used to

https://doi.org/10.1021/jacs.2c12893
J. Am. Chem. Soc. XXXX, XXX, XXX−XXX

deliver mCherry mRNA to trophoblasts, endothelial cells, and immune cells in the placenta. When evaluating VEGF mRNA as a clinically relevant cargo for placental vasodilation, LNP A4 increased VEGFR1 expression and vasodilation of fetal blood vessels in the placenta with a better safety profile than benchmark C12-200 LNPs. Future directions to clinically translate this work will involve the evaluation of the LNP A4 mRNA delivery platform in a murine model of placental insufficiency. Clinical outcomes, such as maternal blood pressure, serum levels of sFlt-1, placental inflammation, placental and fetal weight, and fetal survival, can be quantified as measures of mitigating both the maternal symptoms of pre-eclampsia and the fetal symptoms of FGR. However, there is no clear consensus in the literature on comprehensive models of pre-eclampsia and FGR that capitulate the complex and multisystem effects of these disorders.[69−71] For example, different models have been utilized to mimic particular hallmarks of the disorder, including placental ischemia, placental inflammation, and restricted fetal growth. Therefore, the necessity of multiple models of placental insufficiency to robustly characterize the therapeutic effect of LNP-mediated VEGF mRNA delivery places this work outside the scope of the current study. In conclusion, this work demonstrates the potential of an mRNA LNP platform for protein replacement therapies to treat placental insufficiency disorders.

■ ASSOCIATED CONTENT

Supporting Information

The Supporting Information is available free of charge at https://pubs.acs.org/doi/10.1021/jacs.2c12893.

Materials and methods; LC-MS spectra of ionizable lipids; chemical structures for C12-200 and DLin-MC3-DMA ionizable lipids, LNP-mediated luciferase mRNA delivery to the maternal organs in nonpregnant mice, LNP-mediated luciferase mRNA delivery to the maternal organs in pregnant mice, LNP-mediated mRNA delivery to the placentas and fetuses in pregnant mice, comparing luciferase mRNA delivery to the organs in nonpregnant and pregnant mice, representative flow gating scheme, serum and liver VEGF levels from pregnant mice treated with LNPs A4 and C12-200 encapsulating control mRNA, IHC for VEGFR2 on placentas from pregnant mice treated with VEGF mRNA, and H&E on placentas from pregnant mice treated with VEGF mRNA (PDF)

■ AUTHOR INFORMATION

Corresponding Author

Michael J. Mitchell − *Department of Bioengineering, University of Pennsylvania, Philadelphia, Pennsylvania 19104, United States; Abramson Cancer Center, Perelman School of Medicine, Institute for Immunology, Perelman School of Medicine, Cardiovascular Institute, Perelman School of Medicine, and Institute for Regenerative Medicine, Perelman School of Medicine, University of Pennsylvania, Philadelphia, Pennsylvania 19104, United States; Penn Institute for RNA Innovation, Perelman School of Medicine, University of Pennsylvania, Philadelphia 19104, United States;* orcid.org/0000-0002-3628-2244; Email: mjmitch@seas.upenn.edu

Authors

Kelsey L. Swingle − *Department of Bioengineering, University of Pennsylvania, Philadelphia, Pennsylvania 19104, United States;* orcid.org/0000-0001-8475-9206

Hannah C. Safford − *Department of Bioengineering, University of Pennsylvania, Philadelphia, Pennsylvania 19104, United States*

Hannah C. Geisler − *Department of Bioengineering, University of Pennsylvania, Philadelphia, Pennsylvania 19104, United States*

Alex G. Hamilton − *Department of Bioengineering, University of Pennsylvania, Philadelphia, Pennsylvania 19104, United States*

Ajay S. Thatte − *Department of Bioengineering, University of Pennsylvania, Philadelphia, Pennsylvania 19104, United States*

Margaret M. Billingsley − *Department of Bioengineering, University of Pennsylvania, Philadelphia, Pennsylvania 19104, United States;* orcid.org/0000-0003-4499-9066

Ryann A. Joseph − *Department of Bioengineering, University of Pennsylvania, Philadelphia, Pennsylvania 19104, United States;* orcid.org/0000-0002-0795-6094

Kaitlin Mrksich − *Department of Bioengineering, University of Pennsylvania, Philadelphia, Pennsylvania 19104, United States*

Marshall S. Padilla − *Department of Bioengineering, University of Pennsylvania, Philadelphia, Pennsylvania 19104, United States*

Aditi A. Ghalsasi − *Department of Bioengineering, University of Pennsylvania, Philadelphia, Pennsylvania 19104, United States*

Mohamad-Gabriel Alameh − *Department of Medicine, University of Pennsylvania, Philadelphia, Pennsylvania 19104, United States; Penn Institute for RNA Innovation, Perelman School of Medicine, University of Pennsylvania, Philadelphia 19104, United States;* orcid.org/0000-0002-5672-6930

Drew Weissman − *Department of Medicine, University of Pennsylvania, Philadelphia, Pennsylvania 19104, United States; Penn Institute for RNA Innovation, Perelman School of Medicine, University of Pennsylvania, Philadelphia 19104, United States;* orcid.org/0000-0002-1501-6510

Complete contact information is available at: https://pubs.acs.org/10.1021/jacs.2c12893

Funding

M.J.M. acknowledges support from a US National Institutes of Health (NIH) Director's New Innovator Award (DP2 TR002776), a Burroughs Wellcome Fund Career Award at the Scientific Interface (CASI), a US National Science Foundation CAREER Award (CBET-2145491), an American Cancer Society Research Scholar Grant (RSG-22-122-01-ET) and the National Institutes of Health (NCI R01 CA241661, NCI R37 CA244911, and NIDDK R01 DK123049). K.L.S., H.C.S., H.C.G., A.G.H., and A.S.T. acknowledge support from the US National Science Foundation Graduate Research Fellowship. M.M.B. acknowledges support US National Institutes of Health Ruth L. Kirschstein National Research Service Award (F31 CA260922). M.S.P. acknowledges support from the National Institute of Dental and Craniofacial Research of the NIH (T90DE030854). The content is solely the responsibility of the authors and does not necessarily represent the official views of the NIH.

https://doi.org/10.1021/jacs.2c12893
J. Am. Chem. Soc. XXXX, XXX, XXX−XXX

Notes

The authors declare the following competing financial interest(s): K.L.S and M.J.M. have filed a patent application based on this work. M.J.M. is an inventor on a patent related to this work filed by the Trustees of the University of Pennsylvania (PCT/US20/56252). D.W. is an inventor on several patents related to this work filed by the Trustees of the University of Pennsylvania (11/990,646; 13/ 585,517; 13/ 839,023; 13/839,155; 14/456,302; 15/339,363; 16/ 299,202). All other authors declare they have no competing interests.

■ ACKNOWLEDGMENTS

The authors are grateful to Fangping Chen from The Wistar Institute Histotechnology Facility for providing technical support for histological preparation of placental sections. Funding support for The Wistar Institute core facilities was provided by Cancer Center Support Grant P30 CA010815.

■ ABBREVIATIONS

ALT	alanine transaminase
AST	aspartate aminotransferase
CK7	cytokeratin-7
FGR	fetal growth restriction
H&E	hematoxylin and eosin
IVIS	in vivo imaging system
LNP	lipid nanoparticle
mRNA	messenger RNA
PlGF	placental growth factor
sFlt-1	soluble fms-like tyrosine kinase
TGCs	trophoblast giant cells
VEGF	vascular endothelial growth factor
VEGFR1	vascular endothelial growth factor receptor 1
VEGFR2	vascular endothelial growth factor receptor 2

■ REFERENCES

(1) Kauffman, K. J.; Webber, M. J.; Anderson, D. G. Materials for Non-Viral Intracellular Delivery of Messenger RNA Therapeutics. *J. Controlled Release* **2016**, *240*, 227−234.

(2) Swingle, K. L.; Hamilton, A. G.; Mitchell, M. J. Lipid Nanoparticle-Mediated Delivery of MRNA Therapeutics and Vaccines. *Trends Mol. Med.* **2021**, *27*, 616−617.

(3) Giacca, M.; Zacchigna, S. Virus-Mediated Gene Delivery for Human Gene Therapy. *J. Controlled Release* **2012**, *161*, 377−388.

(4) Howe, S. J.; Mansour, M. R.; Schwarzwaelder, K.; Bartholomae, C.; Hubank, M.; Kempski, H.; Brugman, M. H.; Pike-Overzet, K.; Chatters, S. J.; de Ridder, D.; Gilmour, K. C.; Adams, S.; Thornhill, S. I.; Parsley, K. L.; Staal, F. J. T.; Gale, R. E.; Linch, D. C.; Bayford, J.; Brown, L.; Quaye, M.; Kinnon, C.; Ancliff, P.; Webb, D. K.; Schmidt, M.; von Kalle, C.; Gaspar, H. B.; Thrasher, A. J. Insertional Mutagenesis Combined with Acquired Somatic Mutations Causes Leukemogenesis Following Gene Therapy of SCID-X1 Patients. *J. Clin. Invest.* **2008**, *118*, 3143−3150.

(5) Yin, H.; Kanasty, R. L.; Eltoukhy, A. A.; Vegas, A. J.; Dorkin, J. R.; Anderson, D. G. Non-Viral Vectors for Gene-Based Therapy. *Nat. Rev. Genet.* **2014**, *15*, 541−555.

(6) Hajj, K. A.; Whitehead, K. A. Tools for Translation: Non-Viral Materials for Therapeutic MRNA Delivery. *Nat. Rev. Mater.* **2017**, *2*, 17056.

(7) Kowalski, P. S.; Rudra, A.; Miao, L.; Anderson, D. G. Delivering the Messenger: Advances in Technologies for Therapeutic MRNA Delivery. *Mol. Ther.* **2019**, *27*, 710−728.

(8) Hajj, K. A.; Melamed, J. R.; Chaudhary, N.; Lamson, N. G.; Ball, R. L.; Yerneni, S. S.; Whitehead, K. A. A Potent Branched-Tail Lipid Nanoparticle Enables Multiplexed MRNA Delivery and Gene Editing In Vivo. *Nano Lett.* **2020**, *20*, 5167−5175.

(9) Kauffman, K. J.; Dorkin, J. R.; Yang, J. H.; Heartlein, M. W.; DeRosa, F.; Mir, F. F.; Fenton, O. S.; Anderson, D. G. Optimization of Lipid Nanoparticle Formulations for MRNA Delivery in Vivo with Fractional Factorial and Definitive Screening Designs. *Nano Lett.* **2015**, *15*, 7300−7306.

(10) Oberli, M. A.; Reichmuth, A. M.; Dorkin, J. R.; Mitchell, M. J.; Fenton, O. S.; Jaklenec, A.; Anderson, D. G.; Langer, R.; Blankschtein, D. Lipid Nanoparticle Assisted MRNA Delivery for Potent Cancer Immunotherapy. *Nano Lett.* **2017**, *17*, 1326−1335.

(11) Fenton, O. S.; Kauffman, K. J.; Kaczmarek, J. C.; McClellan, R. L.; Jhunjhunwala, S.; Tibbitt, M. W.; Zeng, M. D.; Appel, E. A.; Dorkin, J. R.; Mir, F. F.; Yang, J. H.; Oberli, M. A.; Heartlein, M. W.; DeRosa, F.; Langer, R.; Anderson, D. G. Synthesis and Biological Evaluation of Ionizable Lipid Materials for the In Vivo Delivery of Messenger RNA to B Lymphocytes. *Adv. Mater.* **2017**, *29*, No. 1606944.

(12) Tao, W.; Peppas, N. A. Robotic Pills for Gastrointestinal-Tract-Targeted Oral MRNA Delivery. *Matter* **2022**, *5*, 775−777.

(13) Xiao, Y.; Tang, Z.; Huang, X.; Chen, W.; Zhou, J.; Liu, H.; Liu, C.; Kong, N.; Tao, W. Emerging MRNA Technologies: Delivery Strategies and Biomedical Applications. *Chem. Soc. Rev.* **2022**, *51*, 3828−3845.

(14) Jackson, L. A.; Anderson, E. J.; Rouphael, N. G.; Roberts, P. C.; Makhene, M.; Coler, R. N.; McCullough, M. P.; Chappell, J. D.; Denison, M. R.; Stevens, L. J.; Pruijssers, A. J.; McDermott, A.; Flach, B.; Doria-Rose, N. A.; Corbett, K. S.; Morabito, K. M.; O'Dell, S.; Schmidt, S. D.; Swanson, P. A.; Padilla, M.; Mascola, J. R.; Neuzil, K. M.; Bennett, H.; Sun, W.; Peters, E.; Makowski, M.; Albert, J.; Cross, K.; Buchanan, W.; Pikaart-Tautges, R.; Ledgerwood, J. E.; Graham, B. S.; Beigel, J. H. An MRNA Vaccine against SARS-CoV-2 — Preliminary Report. *N. Engl. J. Med.* **2020**, *383*, 1920−1931.

(15) Vogel, A. B.; Kanevsky, I.; Che, Y.; Swanson, K. A.; Muik, A.; Vormehr, M.; Kranz, L. M.; Walzer, K. C.; Hein, S.; Güler, A.; Loschko, J.; Maddur, M. S.; Ota-Setlik, A.; Tompkins, K.; Cole, J.; Lui, B. G.; Ziegenhals, T.; Plaschke, A.; Eisel, D.; Dany, S. C.; Fesser, S.; Erbar, S.; Bates, F.; Schneider, D.; Jesionek, B.; Sänger, B.; Wallisch, A.-K.; Feuchter, Y.; Junginger, H.; Krumm, S. A.; Heinen, A. P.; Adams-Quack, P.; Schlereth, J.; Schille, S.; Kröner, C.; de la Caridad Güimil Garcia, R.; Hiller, T.; Fischer, L.; Sellers, R. S.; Choudhary, S.; Gonzalez, O.; Vascotto, F.; Gutman, M. R.; Fontenot, J. A.; Hall-Ursone, S.; Brasky, K.; Griffor, M. C.; Han, S.; Su, A. A. H.; Lees, J. A.; Nedoma, N. L.; Mashalidis, E. H.; Sahasrabudhe, P. V.; Tan, C. Y.; Pavliakova, D.; Singh, G.; Fontes-Garfias, C.; Pride, M.; Scully, I. L.; Ciolino, T.; Obregon, J.; Gazi, M.; Carrion, R.; Alfson, K. J.; Kalina, W. V.; Kaushal, D.; Shi, P.-Y.; Klamp, T.; Rosenbaum, C.; Kuhn, A. N.; Türeci, Ö.; Dormitzer, P. R.; Jansen, K. U.; Sahin, U. Immunogenic BNT162b Vaccines Protect Rhesus Macaques from SARS-CoV-2. *Nature* **2021**, *592*, 283−289.

(16) Gillmore, J. D.; Gane, E.; Taubel, J.; Kao, J.; Fontana, M.; Maitland, M. L.; Seitzer, J.; O'Connell, D.; Walsh, K. R.; Wood, K.; Phillips, J.; Xu, Y.; Amaral, A.; Boyd, A. P.; Cehelsky, J. E.; McKee, M. D.; Schiermeier, A.; Harari, O.; Murphy, A.; Kyratsous, C. A.; Zambrowicz, B.; Soltys, R.; Gutstein, D. E.; Leonard, J.; Sepp-Lorenzino, L.; Lebwohl, D. CRISPR-Cas9 In Vivo Gene Editing for Transthyretin Amyloidosis. *N. Engl. J. Med.* **2021**, *385*, 493−502.

(17) Knöfler, M.; Haider, S.; Saleh, L.; Pollheimer, J.; Gamage, T. K. J. B.; James, J. Human Placenta and Trophoblast Development: Key Molecular Mechanisms and Model Systems. *Cell. Mol. Life Sci.* **2019**, *76*, 3479−3496.

(18) Aplin, J. D.; Myers, J. E.; Timms, K.; Westwood, M. Tracking Placental Development in Health and Disease. *Nat. Rev. Endocrinol.* **2020**, *16*, 479−494.

(19) Chappell, L. C.; Cluver, C. A.; Kingdom, J.; Tong, S. Pre-Eclampsia. *Lancet* **2021**, *398*, 341−354.

(20) Woods, L.; Perez-Garcia, V.; Hemberger, M. Regulation of Placental Development and Its Impact on Fetal Growth—New Insights From Mouse Models. *Front. Endocrinol.* **2018**, *9*, No. 570.

https://doi.org/10.1021/jacs.2c12893
J. Am. Chem. Soc. XXXX, XXX, XXX−XXX

(21) David, A. L. Maternal Uterine Artery VEGF Gene Therapy for Treatment of Intrauterine Growth Restriction. *Placenta* **2017**, *59*, S44−S50.
(22) Mehta, V.; Abi-Nader, K. N.; Peebles, D. M.; Benjamin, E.; Wigley, V.; Torondel, B.; Filippi, E.; Shaw, S. W.; Boyd, M.; Martin, J.; Zachary, I.; David, A. L. Long-Term Increase in Uterine Blood Flow Is Achieved by Local Overexpression of VEGF-A 165 in the Uterine Arteries of Pregnant Sheep. *Gene Ther.* **2012**, *19*, 925−935.
(23) Swanson, A. M.; Rossi, C. A.; Ofir, K.; Mehta, V.; Boyd, M.; Barker, H.; Ledwozyw, A.; Vaughan, O.; Martin, J.; Zachary, I.; Sebire, N.; Peebles, D. M.; David, A. L. Maternal Therapy with Ad.VEGF-A165 Increases Fetal Weight at Term in a Guinea-Pig Model of Fetal Growth Restriction. *Hum. Gene Ther.* **2016**, *27*, 997−1007.
(24) David, A. L.; Torondel, B.; Zachary, I.; Wigley, V.; Nader, K. A.; Mehta, V.; Buckley, S. M. K.; Cook, T.; Boyd, M.; Rodeck, C. H.; Martin, J.; Peebles, D. M. Local Delivery of VEGF Adenovirus to the Uterine Artery Increases Vasorelaxation and Uterine Blood Flow in the Pregnant Sheep. *Gene Ther.* **2008**, *15*, 1344−1350.
(25) Young, R. E.; Nelson, K. M.; Hofbauer, S. I.; Vijayakumar, T.; Alameh, M.-G.; Weissman, D.; Papachristou, C.; Gleghorn, J. P.; Riley, R. S. Lipid Nanoparticle Composition Drives MRNA Delivery to the Placenta. *bioRxiv* December 22, 2022, https://doi.org/10.1101/2022.12.22.521490.
(26) Cheng, Q.; Wei, T.; Jia, Y.; Farbiak, L.; Zhou, K.; Zhang, S.; Wei, Y.; Zhu, H.; Siegwart, D. J. Dendrimer-Based Lipid Nanoparticles Deliver Therapeutic FAH MRNA to Normalize Liver Function and Extend Survival in a Mouse Model of Hepatorenal Tyrosinemia Type I. *Adv. Mater.* **2018**, *30*, No. 1805308.
(27) Turanov, A. A.; Lo, A.; Hassler, M. R.; Makris, A.; Ashar-Patel, A.; Alterman, J. F.; Coles, A. H.; Haraszti, R. A.; Roux, L.; Godinho, B. M.; Echeverria, D.; Pears, S.; Iliopoulos, J.; Shanmugalingam, R.; Ogle, R.; Zsengeller, Z. K.; Hennessy, A.; Karumanchi, S. A.; Moore, M. J.; Khvorova, A. RNAi Modulation of Placental SFLT1 for the Treatment of Preeclampsia. *Nat. Biotechnol.* **2018**, *36*, 1164−1173.
(28) Witzigmann, D.; Kulkarni, J. A.; Leung, J.; Chen, S.; Cullis, P. R.; van der Meel, R. Lipid Nanoparticle Technology for Therapeutic Gene Regulation in the Liver. *Adv. Drug Delivery Rev.* **2020**, *159*, 344−363.
(29) Carter, A. M. Animal Models of Human Pregnancy and Placentation: Alternatives to the Mouse. *Reproduction* **2020**, *160*, R129−R143.
(30) Chen, D.; Love, K. T.; Chen, Y.; Eltoukhy, A. A.; Kastrup, C.; Sahay, G.; Jeon, A.; Dong, Y.; Whitehead, K. A.; Anderson, D. G. Rapid Discovery of Potent SiRNA-Containing Lipid Nanoparticles Enabled by Controlled Microfluidic Formulation. *J. Am. Chem. Soc.* **2012**, *134*, 6948−6951.
(31) Jayaraman, M.; Ansell, S. M.; Mui, B. L.; Tam, Y. K.; Chen, J.; Du, X.; Butler, D.; Eltepu, L.; Matsuda, S.; Narayanannair, J. K.; Rajeev, K. G.; Hafez, I. M.; Akinc, A.; Maier, M. A.; Tracy, M. A.; Cullis, P. R.; Madden, T. D.; Manoharan, M.; Hope, M. J. Maximizing the Potency of SiRNA Lipid Nanoparticles for Hepatic Gene Silencing In Vivo. *Angew. Chem.* **2012**, *124*, 8657−8661.
(32) Whitehead, K. A.; Dorkin, J. R.; Vegas, A. J.; Chang, P. H.; Veiseh, O.; Matthews, J.; Fenton, O. S.; Zhang, Y.; Olejnik, K. T.; Yesilyurt, V.; Chen, D.; Barros, S.; Klebanov, B.; Novobrantseva, T.; Langer, R.; Anderson, D. G. Degradable Lipid Nanoparticles with Predictable in Vivo SiRNA Delivery Activity. *Nat. Commun.* **2014**, *5*, No. 4277.
(33) Han, X.; Zhang, H.; Butowska, K.; Swingle, K. L.; Alameh, M.-G.; Weissman, D.; Mitchell, M. J. An Ionizable Lipid Toolbox for RNA Delivery. *Nat. Commun.* **2021**, *12*, No. 7233.
(34) Orendi, K.; Kivity, V.; Sammar, M.; Grimpel, Y.; Gonen, R.; Meiri, H.; Lubzens, E.; Huppertz, B. Placental and Trophoblastic in Vitro Models to Study Preventive and Therapeutic Agents for Preeclampsia. *Placenta* **2011**, *32*, S49−S54.
(35) Umapathy, A.; Chamley, L. W.; James, J. L. Reconciling the Distinct Roles of Angiogenic/Anti-Angiogenic Factors in the Placenta and Maternal Circulation of Normal and Pathological Pregnancies. *Angiogenesis* **2020**, *23*, 105−117.
(36) Krishnan, T.; David, A. L. Placenta-Directed Gene Therapy for Fetal Growth Restriction. *Semin. Fetal Neonatal Med.* **2017**, *22*, 415−422.
(37) Cardarelli, F.; Digiacomo, L.; Marchini, C.; Amici, A.; Salomone, F.; Fiume, G.; Rossetta, A.; Gratton, E.; Pozzi, D.; Caracciolo, G. The Intracellular Trafficking Mechanism of Lipofectamine-Based Transfection Reagents and Its Implication for Gene Delivery. *Sci. Rep.* **2016**, *6*, No. 25879.
(38) Wang, T.; Larcher, L. M.; Ma, L.; Veedu, R. N. Systematic Screening of Commonly Used Commercial Transfection Reagents towards Efficient Transfection of Single-Stranded Oligonucleotides. *Molecules* **2018**, *23*, 2564.
(39) Cheng, Q.; Wei, T.; Farbiak, L.; Johnson, L. T.; Dilliard, S. A.; Siegwart, D. J. Selective Organ Targeting (SORT) Nanoparticles for Tissue-Specific MRNA Delivery and CRISPR−Cas Gene Editing. *Nat. Nanotechnol.* **2020**, *15*, 313−320.
(40) Paunovska, K.; Sago, C. D.; Monaco, C. M.; Hudson, W. H.; Castro, M. G.; Rudoltz, T. G.; Kalathoor, S.; Vanover, D. A.; Santangelo, P. J.; Ahmed, R.; Bryksin, A. V.; Dahlman, J. E. A Direct Comparison of in Vitro and in Vivo Nucleic Acid Delivery Mediated by Hundreds of Nanoparticles Reveals a Weak Correlation. *Nano Lett.* **2018**, *18*, 2148−2157.
(41) Chen, S.; Tam, Y. Y. C.; Lin, P. J. C.; Sung, M. M. H.; Tam, Y. K.; Cullis, P. R. Influence of Particle Size on the in Vivo Potency of Lipid Nanoparticle Formulations of SiRNA. *J. Controlled Release* **2016**, *235*, 236−244.
(42) Semmler-Behnke, M.; Lipka, J.; Wenk, A.; Hirn, S.; Schäffler, M.; Tian, F.; Schmid, G.; Oberdörster, G.; Kreyling, W. G. Size Dependent Translocation and Fetal Accumulation of Gold Nanoparticles from Maternal Blood in the Rat. *Part. Fibre Toxicol.* **2014**, *11*, 33.
(43) Irvin-Choy, N. S.; Nelson, K. M.; Dang, M. N.; Gleghorn, J. P.; Day, E. S. Gold Nanoparticle Biodistribution in Pregnant Mice Following Intravenous Administration Varies with Gestational Age. *Nanomed.: Nanotechnol., Biol. Med.* **2021**, *36*, No. 102412.
(44) Paul, J. W.; Hua, S.; Ilicic, M.; Tolosa, J. M.; Butler, T.; Robertson, S.; Smith, R. Drug Delivery to the Human and Mouse Uterus Using Immunoliposomes Targeted to the Oxytocin Receptor. *Am. J. Obstet. Gynecol.* **2017**, *216*, 283.
(45) Alfaifi, A. A.; Heyder, R. S.; Bielski, E. R.; Almuqbil, R. M.; Kavdia, M.; Gerk, P. M.; da Rocha, S. R. P. Megalin-Targeting Liposomes for Placental Drug Delivery. *J. Controlled Release* **2020**, *324*, 366−378.
(46) Ho, D.; Leong, J. W.; Crew, R. C.; Norret, M.; House, M. J.; Mark, P. J.; Waddell, B. J.; Iyer, K. S.; Keelan, J. A. Maternal-Placental-Fetal Biodistribution of Multimodal Polymeric Nanoparticles in a Pregnant Rat Model in Mid and Late Gestation. *Sci. Rep.* **2017**, *7*, No. 2866.
(47) Kertschanska, S.; Stulcová, B.; Kaufmann, P.; Stulc, J. Distensible Transtrophoblastic Channels in the Rat Placenta. *Placenta* **2000**, *21*, 670−677.
(48) Kertschanska, S.; Kosanke, G.; Kaufmann, P. Pressure Dependence of So-Called Transtrophoblastic Channels during Fetal Perfusion of Human Placental Villi. *Microsc. Res. Tech.* **1997**, *38*, 52−62.
(49) Sanghavi, M.; Rutherford, J. D. Cardiovascular Physiology of Pregnancy. *Circulation* **2014**, *130*, 1003−1008.
(50) Frederiksen, M. C. Physiologic Changes in Pregnancy and Their Effect on Drug Disposition. *Semin. Perinatol.* **2001**, *25*, 120−123.
(51) Pennington, K. A.; Schlitt, J. M.; Schulz, L. C. Isolation of Primary Mouse Trophoblast Cells and Trophoblast Invasion Assay. *J. Vis. Exp.* **2012**, *59*, No. e3202.
(52) Maldonado-Estrada, J.; Menu, E.; Roques, P.; Barré-Sinoussi, F.; Chaouat, G. Evaluation of Cytokeratin 7 as an Accurate Intracellular Marker with Which to Assess the Purity of Human Placental Villous Trophoblast Cells by Flow Cytometry. *J. Immunol. Methods* **2004**, *286*, 21−34.

https://doi.org/10.1021/jacs.2c12893
J. Am. Chem. Soc. XXXX, XXX, XXX−XXX

(53) Dunk, C.; Kwan, M.; Hazan, A.; Walker, S.; Wright, J. K.; Harris, L. K.; Jones, R. L.; Keating, S.; Kingdom, J. C. P.; Whittle, W.; Maxwell, C.; Lye, S. J. Failure of Decidualization and Maternal Immune Tolerance Underlies Uterovascular Resistance in Intra Uterine Growth Restriction. *Front. Endocrinol.* **2019**, *10*, No. 160.
(54) Kheirolomoom, A.; Kare, A. J.; Ingham, E. S.; Paulmurugan, R.; Robinson, E. R.; Baikoghli, M.; Inayathullah, M.; Seo, J. W.; Wang, J.; Fite, B. Z.; Wu, B.; Tumbale, S. K.; Raie, M. N.; Cheng, R. H.; Nichols, L.; Borowsky, A. D.; Ferrara, K. W. In Situ T-Cell Transfection by Anti-CD3-Conjugated Lipid Nanoparticles Leads to T-Cell Activation, Migration, and Phenotypic Shift. *Biomaterials* **2022**, *281*, No. 121339.
(55) Siddiqui, A. H.; Irani, R. A.; Zhang, Y.; Dai, Y.; Blackwell, S. C.; Ramin, S. M.; Kellems, R. E.; Xia, Y. Recombinant Vascular Endothelial Growth Factor 121 Attenuates Autoantibody-Induced Features of Pre-Eclampsia in Pregnant Mice. *Am. J. Hypertens.* **2011**, *24*, 606−612.
(56) AstraZeneca. *A Randomized, Double-Blind, Placebo-Controlled, Multi-Centre, Sequential Design, Phase IIa Study to Evaluate Safety and Tolerability of Epicardial Injections of AZD8601 During Coronary Artery Bypass Grafting Surgery; Clinical Trial Registration NCT03370887*, 2021.
(57) Anttila, V.; Saraste, A.; Knuuti, J.; Jaakkola, P.; Hedman, M.; Svedlund, S.; Lagerström-Fermér, M.; Kjaer, M.; Jeppsson, A.; Gan, L.-M. Synthetic MRNA Encoding VEGF-A in Patients Undergoing Coronary Artery Bypass Grafting: Design of a Phase 2a Clinical Trial. *Mol. Ther. − Methods Clin. Dev.* **2020**, *18*, 464−472.
(58) Shibuya, M. Vascular Endothelial Growth Factor Receptor-1 (VEGFR-1/Flt-1): A Dual Regulator for Angiogenesis. *Angiogenesis* **2006**, *9*, 225−230.
(59) Pietro, L.; Daher, S.; Rudge, M. V. C.; Calderon, I. M. P.; Damasceno, D. C.; Sinzato, Y. K.; Bandeira, C.; Bevilacqua, E. Vascular Endothelial Growth Factor (VEGF) and VEGF-Receptor Expression in Placenta of Hyperglycemic Pregnant Women. *Placenta* **2010**, *31*, 770−780.
(60) Riley, R. S.; Kashyap, M. V.; Billingsley, M. M.; White, B.; Alameh, M.-G.; Bose, S. K.; Zoltick, P. W.; Li, H.; Zhang, R.; Cheng, A. Y.; Weissman, D.; Peranteau, W. H.; Mitchell, M. J. Ionizable Lipid Nanoparticles for in Utero MRNA Delivery. *Sci. Adv.* **2021**, *7*, No. eaba1028.
(61) Kauffman, K. J.; Mir, F. F.; Jhunjhunwala, S.; Kaczmarek, J. C.; Hurtado, J. E.; Yang, J. H.; Webber, M. J.; Kowalski, P. S.; Heartlein, M. W.; DeRosa, F.; Anderson, D. G. Efficacy and Immunogenicity of Unmodified and Pseudouridine-Modified MRNA Delivered Systemically with Lipid Nanoparticles in Vivo. *Biomaterials* **2016**, *109*, 78−87.
(62) Simón-Yarza, T.; Formiga, F. R.; Tamayo, E.; Pelacho, B.; Prosper, F.; Blanco-Prieto, M. J. Vascular Endothelial Growth Factor-Delivery Systems for Cardiac Repair: An Overview. *Theranostics* **2012**, *2*, 541−552.
(63) Rennel, E. S.; Hamdollah-Zadeh, M. A.; Wheatley, E. R.; Magnussen, A.; Schüler, Y.; Kelly, S. P.; Finucane, C.; Ellison, D.; Cebe-Suarez, S.; Ballmer-Hofer, K.; Mather, S.; Stewart, L.; Bates, D. O.; Harper, S. J. Recombinant Human VEGF165b Protein Is an Effective Anti-Cancer Agent in Mice. *Eur. J. Cancer* **2008**, *44*, 1883−1894.
(64) Hsu, S.-h.; Yu, B.; Wang, X.; Lu, Y.; Schmidt, C. R.; Lee, R. J.; Lee, L. J.; Jacob, S. T.; Ghoshal, K. Cationic Lipid Nanoparticles for Therapeutic Delivery of SiRNA and MiRNA to Murine Liver Tumor. *Nanomed.: Nanotechnol., Biol. Med.* **2013**, *9*, 1169−1180.
(65) Guan, C.; Zhao, F.; Yang, Z.; Tang, Q.; Wang, L.; Li, X.; Zhang, L.; Deng, Z.; Hou, H.; Wang, J.; Xu, Y.; Zhang, R.; Lin, Y.; Tan, P.; Zhang, Y.; Liu, S.; Zhang, L. A Review of Key Cytokines Based on Gene Polymorphism in the Pathogenesis of Pre-Eclampsia. *Am. J. Reprod. Immunol.* **2022**, *87*, No. e13503.
(66) Hu, J.; Wang, H.; Hu, Y.-F.; Xu, X.-F.; Chen, Y.-H.; Xia, M.-Z.; Zhang, C.; Xu, D.-X. Cadmium Induces Inflammatory Cytokines through Activating Akt Signaling in Mouse Placenta and Human Trophoblast Cells. *Placenta* **2018**, *65*, 7−14.
(67) Papuchova, H.; Latos, P. A. Transcription Factor Networks in Trophoblast Development. *Cell. Mol. Life Sci.* **2022**, *79*, 337.
(68) Kaneko-Ishino, T.; Ishino, F. The Role of Genes Domesticated from LTR Retrotransposons and Retroviruses in Mammals. *Front. Microbiol.* **2012**, *3*, 262.
(69) Waker, C. A.; Kaufman, M. R.; Brown, T. L. Current State of Preeclampsia Mouse Models: Approaches, Relevance, and Standardization. *Front. Physiol.* **2021**, *12*, No. 681632.
(70) McCarthy, F. P.; Kingdom, J. C.; Kenny, L. C.; Walsh, S. K. Animal Models of Preeclampsia; Uses and Limitations. *Placenta* **2011**, *32*, 413−419.
(71) Gatford, K. L.; Andraweera, P. H.; Roberts, C. T.; Care, A. S. Animal Models of Preeclampsia. *Hypertension* **2020**, *75*, 1363−1381.

https://doi.org/10.1021/jacs.2c12893
J. Am. Chem. Soc. XXXX, XXX, XXX−XXX